

**MODELING, SIMULATION AND ANALYSIS OF AN INDIRECT VECTOR
CONTROLLED INDUCTION MOTOR DRIVE**

by

Ramesh V. Kanekal

Thesis submitted to the Faculty of the
Virginia Polytechnic Institute and State University
in partial fulfillment of the requirements for the degree of
Master of Science
in
Electrical Engineering

APPROVED:

Krishnan Ramu, Chairman

William A. Blackwell

Saifur Rahman

20 November 1987

Blacksburg, Virginia

MODELING, SIMULATION AND ANALYSIS OF AN INDIRECT VECTOR CONTROLLED INDUCTION MOTOR DRIVE

by

Ramesh V. Kanekal

Krishnan Ramu, Chairman

Electrical Engineering

(ABSTRACT)

Vector control technique is being widely used in ac motors drives for precise dynamic control of torque, speed and position. The application of vector control scheme to the induction motor drive and the complete modeling, analysis and simulation of the drive system are presented in this thesis. State space models of the motor and the speed controller and the real time models of the inverter switches and the vector controller are integrated to model the drive. Performance differences due to the use of PWM and hysteresis current controllers are examined. Simulation results of the torque and speed drive systems are given. The drive system is linearised around an operating point and the small signal response is evaluated.

Acknowledgements

I wish to express my sincere gratitude to Dr. Krishnan Ramu, whose encouragement, support and guidance from the beginning of the project till the end were tremendous. Chapter 2 of this thesis is taken from his forthcoming text book, Analysis of Electronically controlled Machines. I would like to thank him for allowing me to do so.

I would like to thank Dr. William A. Blackwell and Dr. Saifur Rahman for kindly consenting to be on my graduate committee.

I would like to thank _____ and _____ for their support and suggestions.

Table of Contents

1.0 INTRODUCTION	1
1.1 Vector Control Scheme	1
1.2 Modeling of the vector controlled induction motor drive	2
1.3 Simulation and Analysis	3
1.4 Small signal frequency domain analysis	3
1.5 Objectives of the thesis	4
1.6 Organization of the thesis	4
2.0 VECTOR CONTROL SCHEME	5
2.1 Introduction	5
2.2 Background	5
2.3 Separately Excited DC Motor	6
2.4 Steady State Analysis of Induction Motor	8
2.5 Vector Control Principle	10
2.6 Classification of Vector Control Schemes	13
2.7 Indirect Vector Controller	15
2.8 Tuning of Vector Controller	19

3.0 MODELING OF VECTOR CONTROLLED INDUCTION MOTOR	23
3.1 Introduction	23
3.2 Model of the induction motor	23
3.3 Model of the inverter	23
3.3.1 Hysteresis Current Controller	25
3.3.2 PWM Current Controller	27
3.4 Model of the Vector Controller	29
3.5 The speed controller	30
4.0 SIMULATION AND ANALYSIS	32
4.1 Introduction	32
4.2 Torque drive system	32
4.2.1 Comparison between PWM and Hysteresis Current Controllers.	37
4.3 Speed drive system	40
5.0 SMALL SIGNAL FREQUENCY DOMAIN ANALYSIS	47
5.1 Introduction	47
5.2 The small signal model	48
5.3 The frequency domain analysis of the torque drive system	51
5.4 The frequency domain analysis of the speed drive system	53
5.4.1 The selection of speed controller gains	57
6.0 CONCLUSIONS	59
6.1 Contributions	60
6.2 Scope for future work	60
Bibliography	61

Appendix A. Induction Motor Parameters	63
Appendix B. List of symbols	64
Appendix C. Listing of Programs	67
VITA	80

List of Illustrations

Figure 1. Schematic of a Separately Excited DC Motor.	7
Figure 2. Steady State Equivalent Circuit of an Induction Motor.	9
Figure 3. Phasor Diagram of an Induction Motor.	11
Figure 4. Control Block Diagram of an Induction Motor Drive.	12
Figure 5. Vector Controlled Induction Motor Drive.	14
Figure 6. Schematic of Indirect Vector Controller.	20
Figure 7. The indirect vector controlled drive system	21
Figure 8. The inverter circuit	24
Figure 9. Comparison of commanded and actual currents	26
Figure 10. PWM controller switching logic	28
Figure 11. Block diagram of the speed controller.	31
Figure 12. Torque drive system	34
Figure 13. Flow chart to simulate the induction motor drive	35
Figure 14. Building up of flux	36
Figure 15. Response of the torque drive system with hysteresis controller	38
Figure 16. Response of the torque drive system with PWM controller	39
Figure 17. Variation of torque pulsations with current window size	41
Figure 18. Response of the speed drive system with hysteresis controller	43
Figure 19. Response of a speed drive system with PWM control	44

Figure 20. Response of the speed drive system with hysteresis control to a step input 45

Figure 21. Response of the speed drive system with PWM controller to step
input 46

Figure 22. Bode plot of actual torque to commanded torque transfer function 52

Figure 23. Transient response of the Torque drive system to a step input 54

Figure 24. Bode plot of actual flux to commanded flux transfer function 55

1.0 INTRODUCTION

Induction motor drives are becoming popular in industries because of their low cost and mechanical robustness. Induction motors have higher torque to inertia ratio, higher peak torque capability and higher power per unit weight than dc motors. These superior characteristics of the induction motor combined with their maintenance-free nature make them attractive for servo applications. Induction motors were not used in high performance applications for a long time because of the lack of control techniques to transform them to equivalent dc motor drives in performance.

1.1 Vector Control Scheme

Vector control scheme transforms the induction motor (more generally, any ac motor) into an equivalent separately excited dc motor for control purposes. This scheme was introduced in early 1970's, but the implementation of the scheme was not possible until recently. Advances in microprocessor technology and switching power devices have facilitated the real time implementation of the vector control scheme. The high speed microprocessor can generate the command voltages/currents with minimum delay. The software stored in the microprocessor helps the designer to tune and test the vector controller easily. The higher switching frequency of the inverter enables the instantaneous control of input currents/voltages to the machine.

Vector control scheme requires the instantaneous position of the rotor flux. This is measured in the direct vector control scheme and is estimated in the indirect vector control scheme. The direct vector control scheme requires Hall effect probes/search coils to measure the flux. This requires modifications to the existing machine. Indirect vector controller uses the the real time model of the machine to estimate the instantaneous position of the rotor flux. This scheme is widely used in induction motor drives.

1.2 Modeling of the vector controlled induction motor drive

The induction motor in the vector controlled drive is fed by an inverter. The study of transient response of the drive system is possible only by the use of the dynamic model of the induction motor. The dynamic model of the motor considers the instantaneous effects of varying voltages/currents, stator frequency and torque disturbances. The three phase induction motor is transformed to an equivalent two phase motor. The differential equations that describe the two phase motor model are developed. This two phase induction motor model is often referred to as the d-q axis model. The real time model of the inverter is also developed. The inverter switching can be controlled by either hysteresis or pulse width modulation (PWM) techniques. Real time models of both these techniques are presented. The inverter switches are assumed to be ideal. Every instant of a power device switching on or off is modelled. The equations that describe the vector controller are derived. The models of the induction motor, vector controller and inverter

are combined to get the mathematical model of the indirect vector controlled drive system.

1.3 Simulation and Analysis

The dynamic simulation of the entire drive system is one of the key steps in the validation of the design process of motor drive systems. The dynamic models of the motor, the vector controller and the inverter are integrated to obtain the dynamic model of the drive system. The differential equations that describe the drive system are written in state variable form. The simulation of the drive system involves the numerical solution of these differential equations. The transient response of the drive system is obtained from this time domain simulation. Both the torque drive and speed drive systems are simulated. The effects of hysteresis and PWM type of current control in the torque and speed responses are studied.

1.4 Small signal frequency domain analysis

For the small signal study, the nonlinear equations of the induction motor and vector controller are linearised around an operating point. The resulting equations are arranged in state space form and the various system transfer functions are obtained. The stability of the drive system is analysed using the Bode plots of these transfer functions. This analysis is also useful in the design of speed and position controllers. The torque and

speed bandwidths of the drive system are also obtained from the Bode plots of the transfer functions.

1.5 Objectives of the thesis

The objectives of the thesis are :

1. To model the indirect vector controlled induction motor drive.
2. To perform time domain digital simulation of the drive system
3. To analyze the performance of the torque and speed drive systems.

1.6 Organization of the thesis

This thesis is organized as follows. The vector control principle is described in Chapter 2. The modeling of the torque and speed drive systems are presented in Chapter 3. The methods adopted for simulation of the torque and speed drive systems and the results of the same are discussed in that chapter 4. Chapter 5 gives the small signal frequency domain analysis of the vector controlled induction motor drive system. Stability analysis is also presented in that chapter. Results and conclusions are given Chapter 6.

2.0 VECTOR CONTROL SCHEME

2.1 Introduction

The principle of vector control is presented in this chapter, including the derivation of the vector controller. The transformation of the induction motor control to an equivalent dc separately excited motor control is made evident from the equations of the vector controller.

2.2 Background

DC motors were preferred to ac motors for high-performance applications, mainly because of the ease with which they can be controlled. The existence of two separate windings for field and armature makes the control of speed and torque of the dc motor very simple. AC motors are inherently multi-variable, non-linear control plants. The lack of control strategy to transform the induction motor to an equivalent dc separately excited motor prevented their use in high-performance applications demanding precise torque and field control.

The presence of the commutators and brushes in the dc motors introduces several mechanical limitations which restrict their applications. The brushes and commutators not only require continuous maintenance but also limit the maximum speed of the motor.

In addition, the dc motors can not be operated in corrosive or explosive environments thus limiting their use in certain industrial applications.

The vector control scheme was introduced in the early 1970's as a control solution for the ac motor drives. The vector control scheme effectively transforms the ac machine into an equivalent separately excited dc motor.

2.3 Separately Excited DC Motor

The separately excited dc motor accepts two inputs, viz a field current i_f and an armature current i_a to generate a flux ϕ_f and electromagnetic torque T_e . This is schematically shown in Fig 1. The input output relationship is given by the following equations.

$$T_e = K_t i_f i_a \quad (2.1)$$

$$\phi_f = K_f i_f \quad (2.2)$$

where,

K_t is the torque constant of the motor.

K_f is the flux proportional constant.

From these equations it is clear that flux is dependent on field current alone. If field current is held constant, torque is directly proportional to the armature current, i_a . The commutator fixes the angle between the field and armature fluxes at quadrature, thereby maximizing the torque production for a given armature current. The field current i_f and

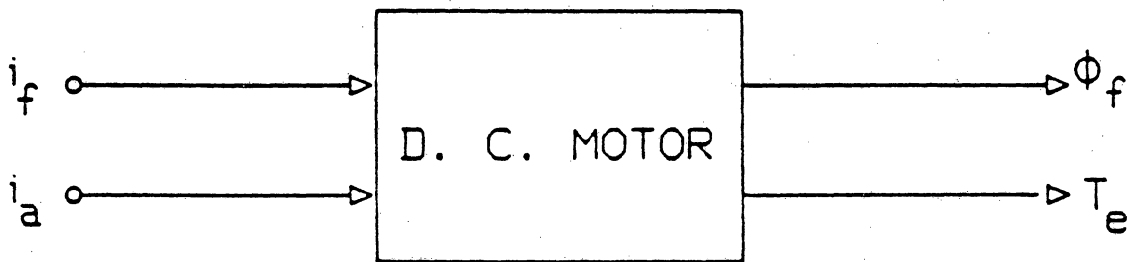


Figure 1. Schematic of a Separately Excited DC Motor.

the armature current i_a are independently controlled. This makes the control of the dc motor very simple.

2.4 Steady State Analysis of Induction Motor

The equivalent circuit of the induction motor is used to analyze the steady state performance of the motor. This circuit is shown in Fig.2. The output torque equation is :

$$T_e = 3 \frac{P}{2} \frac{I_r^2 R_r}{s \omega_s} \quad (2.3)$$

where P is the number of poles, s is the slip, I_r is the rotor current, R_r is the rotor resistance and ω_s is the synchronous frequency.

The flux linkages are given by :

$$\text{Mutual flux linkage} = \psi_m = L_m I_m \quad (2.4)$$

$$\text{Stator flux linkage} = \psi_s = L_m I_m + L_{ls} I_s \quad (2.5)$$

$$\text{Rotor flux linkage} = \psi_r = L_m I_m + L_{lr} I_r \quad (2.6)$$

where, L_m is the mutual inductance, L_{ls} is the stator leakage inductance, L_{lr} is the rotor leakage inductance, I_m is the magnetizing branch current and I_s is the stator current.

From Fig.2. and equations (2.3-2.6), the following points can be noted :

- Both the rotor field flux and torque are controlled through stator phase currents only.

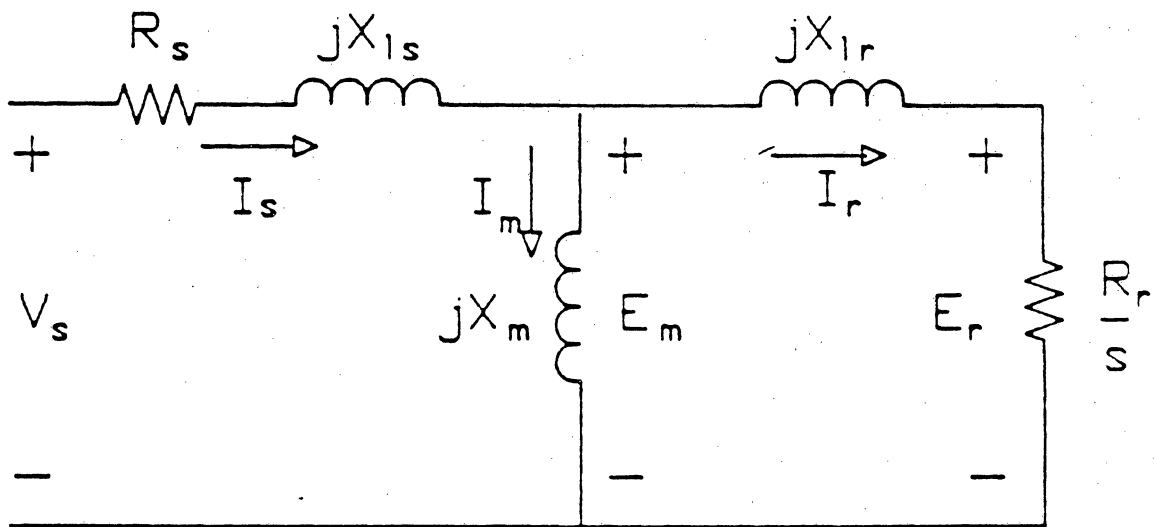


Figure 2. Steady State Equivalent Circuit of an Induction Motor.

- Unlike separately excited dc motor, there are no separate field and armature windings to control the field and torque independently and hence the control becomes complex.

The angle between the rotor flux and stator current θ_T is known as the torque angle and is determined by the load conditions. For an inverter fed induction motor, the phase angle of the current can be controlled with respect to the stator reference frame. This phase angle is the sum of the torque angle and the flux position angle. With load conditions the torque angle changes and hence to adapt to this condition, the phase angle of the current has to be changed accordingly. For this, the knowledge of flux position becomes important. If the flux position with respect to the stator currents is known, accurate control can be achieved by adjusting the phase currents till the required torque angle is obtained.

2.5 Vector Control Principle

If the rotor flux position θ_f is known, then it is possible to resolve the stator current phasor along the rotor flux and in quadrature to it, as shown in Fig.3. The in-phase component is the flux producing current, i_f and the quadrature component is the torque producing current, i_T . If these two components can be controlled independently, then the induction motor control becomes very much similar to the control of a separately excited dc motor. A block diagram of such a control scheme is given in Fig.4. This process of transforming the control of the induction motor to that of an equivalent separately excited dc motor is known as vector control or field oriented control.

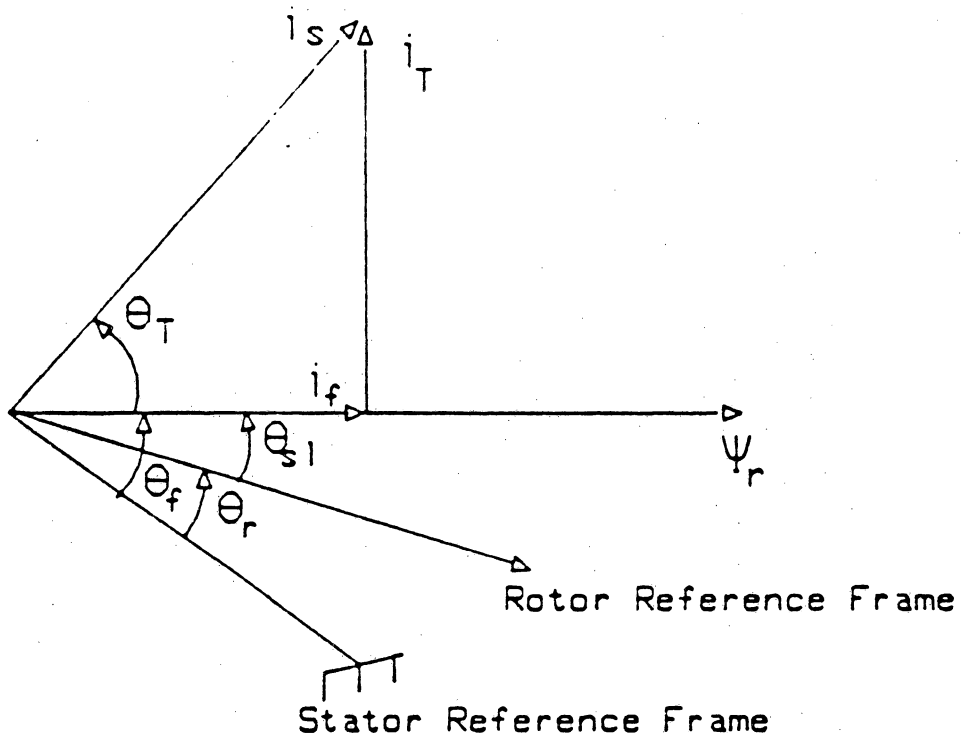


Figure 3. Phasor Diagram of an Induction Motor.

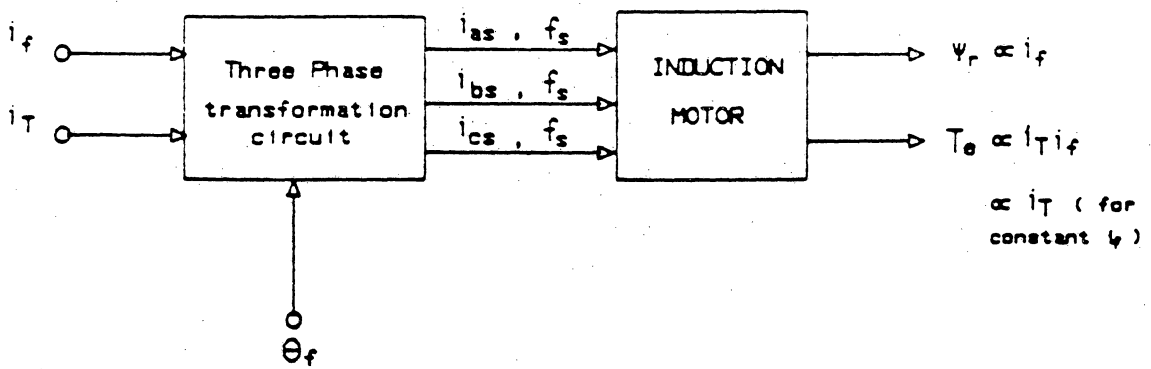


Figure 4. Control Block Diagram of an Induction Motor Drive.

The function of the vector controller is to generate the flux and torque producing current commands from the torque and flux commands. The block diagram of a vector controlled induction motor drive is shown in Fig.5. If the transfer function in the dotted box is given by $G(s)$, then the vector controller has a transfer function of $G^{-1}(s)$, thus making the responses equal to their command values.

2.6 Classification of Vector Control Schemes

For proper implementation of the vector controller, the knowledge of the rotor field angle, θ_r , is crucial. The vector control schemes are classified according to the manner in which this field angle is obtained. The field angle is measured in the direct vector control scheme. The indirect vector controllers estimate the field angle by using a model of the induction motor.

The direct vector control scheme makes use of Hall effect sensors or sensing coils placed near the air gap and embedded in the stator slots to measure instantaneous flux values. From this flux values the field angle is derived. The introduction of Hall sensors or search coils involves modification to existing machine thereby increasing the cost. The Hall sensors are found to be sensitive to temperature and thus are not very reliable. In addition, the sensing coils produce very low voltage at standstill and at low speeds. This impairs the accuracy of measurement. Due to these reasons, the direct vector controller is not very popular. Most of the vector controllers use the indirect vector control scheme.

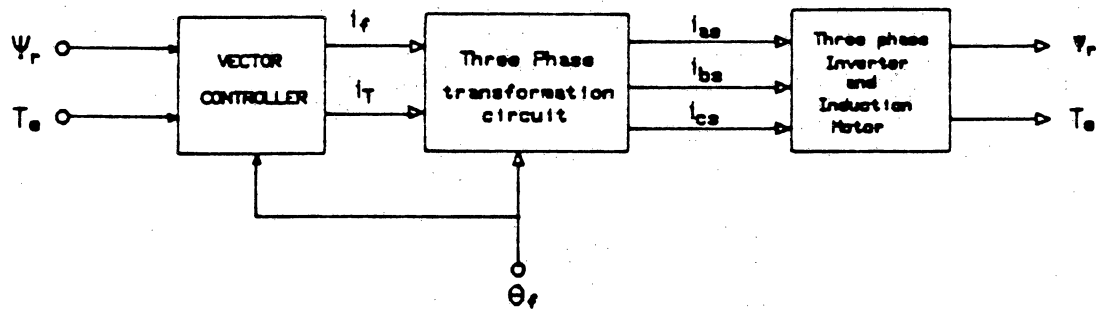


Figure 5. Vector Controlled Induction Motor Drive.

2.7 Indirect Vector Controller

As indicated earlier, the indirect vector controller uses the machine model in order to estimate the rotor flux position. In this section, a step-by-step derivation of the vector controller in dynamic reference frames is given.

The d-q axis equations of an induction motor in synchronously rotating reference frames are given by [11]:

$$\begin{bmatrix} v_{qs}^e \\ v_{ds}^e \\ 0 \\ 0 \end{bmatrix} = \begin{bmatrix} R_s + L_s p & \omega_s L_s & L_m p & \omega_s L_m \\ -\omega_s L_s & R_s + L_s p & -\omega_s L_m & L_m p \\ L_m p & (\omega_s - \omega_r) L_m & R_r + L_r p & (\omega_s - \omega_r) L_r \\ -(\omega_s - \omega_r) L_m & L_m p & -(\omega_s - \omega_r) L_r & R_r + L_r p \end{bmatrix} \begin{bmatrix} i_{qs}^e \\ i_{ds}^e \\ i_{qr}^e \\ i_{dr}^e \end{bmatrix} \quad (2.7)$$

$$T_e = \frac{3}{4} P L_m (i_{qs}^e i_{dr}^e - i_{ds}^e i_{qr}^e) \quad (2.8)$$

$$p\omega_r = \frac{T_e - T_L - B\omega_r}{J} \quad (2.9)$$

where, v_{qs}^e, v_{ds}^e are the stator q and d axes input voltages, i_{qs}^e, i_{ds}^e are the stator q and d axes currents and i_{qr}^e, i_{dr}^e are the rotor q and d axes currents referred to the stator side. R_s and R_r are the stator and referred rotor resistances per phase. L_m is the mutual inductance and L_s and L_r are the stator and referred rotor self-inductances per phase. L_{ls} and L_{lr} are the stator and the referred rotor leakage inductances respectively. ω_s and ω_r are the electrical stator frequency and rotor speed, respectively. T_e is the electromagnetic torque, T_L is the load torque, P is the number of poles, B is the damping factor, J is the moment of inertia and p is the differential operator.

The rotor flux linkages are given by :

$$\psi_{qr} = L_m(i_{qs}^e + i_{qr}^e) + L_{lr}i_{qr}^e \quad (2.10)$$

$$\psi_{dr} = L_m(i_{ds}^e + i_{dr}^e) + L_{lr}i_{dr}^e \quad (2.11)$$

For a voltage source inverter fed induction motor, the voltages v_{qs}^e , v_{ds}^e can be found by a simple transformation from the phase voltages which are input to the system. This transformation is described by Equation (2.12). It should be noted that T_{abc} is a standard transformation matrix which can be used for 3-phase to 2-phase transformation of other variables such as current, flux etc. θ_f is the angle between the stator A phase and the rotor flux position at any time. $\theta_f = \omega_s t$

$$\begin{bmatrix} v_{qs}^e \\ v_{ds}^e \end{bmatrix} = T_{abc} \begin{bmatrix} v_{as} \\ v_{bs} \\ v_{cs} \end{bmatrix} \quad (2.12)$$

where,

$$T_{abc} = \frac{2}{3} \begin{bmatrix} \cos \theta_f & \cos(\theta_f - \frac{2\pi}{3}) & \cos(\theta_f + \frac{2\pi}{3}) \\ \sin \theta_f & \sin(\theta_f - \frac{2\pi}{3}) & \sin(\theta_f + \frac{2\pi}{3}) \end{bmatrix} \quad (2.13)$$

For the present analysis, a current regulated inverter is assumed. The stator currents are maintained at their commanded values, in this type of inverter. The stator currents form the inputs to the system. This has the effect of eliminating stator dynamics from affecting the drive performance. Consequently, the stator equations can be omitted from the system equations. Thus, the rotor equations become,

$$R_r i_{qr}^e + p\psi_{qr}^e + (\omega_s - \omega_r)\psi_{dr} = 0 \quad (2.14)$$

$$R_r i_{dr}^e + p\psi_{dr}^e - (\omega_s - \omega_r)\psi_{qr} = 0 \quad (2.15)$$

Let slip speed ω_{sl} be defined as,

$$\omega_{sl} = \omega_s - \omega_r \quad (2.16)$$

and, let the rotor flux linkage be aligned with the d-axis. Thus,

$$\psi_{dr} = \psi_r \quad (2.17)$$

$$\psi_{qr} = 0 = p\psi_{qr} \quad (2.18)$$

Substituting equations (2.16-2.18) into (2.14-2.15) results in the following rotor equations :

$$R_r i_{qr}^e + \omega_{sl}\psi_r = 0 \quad (2.19)$$

$$R_r i_{dr}^e + p\psi_r = 0 \quad (2.20)$$

The relationship between the stator and the rotor d-q axis currents can be derived by substituting equations (2.17-2.18) into (2.10-2.11),

$$i_{qr}^e = - \frac{L_m}{L_r} i_{qs}^e \quad (2.21)$$

$$i_{dr}^e = \frac{\psi_r}{L_r} - \frac{L_m}{L_r} i_{ds}^e \quad (2.22)$$

If we define the rotor time constant T, as,

$$T_r = \frac{L_r}{R_r} \quad (2.23)$$

the system equations become,

$$\omega_{sl} = \frac{L_m}{T_r} \frac{i_{qs}^e}{\psi_r} \quad (2.24)$$

$$p\psi_r = \frac{1}{T_r} [-\psi_r + L_m i_{ds}^e] \quad (2.25)$$

$$T_e = K_t i_{qs}^e \psi_r \quad (2.26)$$

where,

$$K_t = \frac{3}{2} \frac{P}{2} \frac{L_m}{L_r} \quad (2.27)$$

From these, the torque and flux producing components i_T and i_f can be identified and written as :

$$i_T^* = i_{qs}^{e*} = \frac{2}{3} \frac{2}{P} \frac{T_e^*}{\psi_r^*} \frac{L_r^*}{L_m^*} \quad (2.28)$$

$$i_f^* = i_{ds}^{e*} = \frac{1}{L_m^*} [1 + T_r^* p] \psi_r^* \quad (2.29)$$

The equation for slip speed is,

$$\omega_{sl}^* = \frac{L_m^*}{T_r^*} \frac{i_T^*}{\psi_r^*} \quad (2.30)$$

The quantities marked with asterisk indicate the commanded values and the controller instrumented values. Equations (2.28-2.30) describe the function of indirect vector controller and a schematic of the controller is shown in Fig.6. It can be noted that some proportional terms from equation (2.28) are omitted from the schematic in order to simplify the schematic.

The entire drive system consisting of the motor, inverter and the vector controller is shown in Fig.7. The current and speed loops of the system are closed. The speed command forms the input to the system. The actual speed is sensed and compared with the reference value and the error signal is produced. The speed controller generates the command value of the torque from the speed error signal. The vector controller accepts the torque and flux command values to generate the command values of the stator currents. The current control loop makes the actual currents follow the command values.

2.8 Tuning of Vector Controller

The vector controller uses a model of the machine to estimate the field position angle. The rotor and stator resistances and leakage inductances along with the mutual inductance are the basic elements of the induction motor model. Accurate construction of the stator current vectors from the torque and flux commands is achieved only if the parameters of the vector controller match those of the motor. The parameters of the induction motor change with temperature and saturation. This results in a mismatch between the actual motor parameters and the vector controller parameters. This mismatch can be eliminated by the use of parameter compensation schemes. This thesis work assumes that the parameters of the controller are properly compensated and pro-

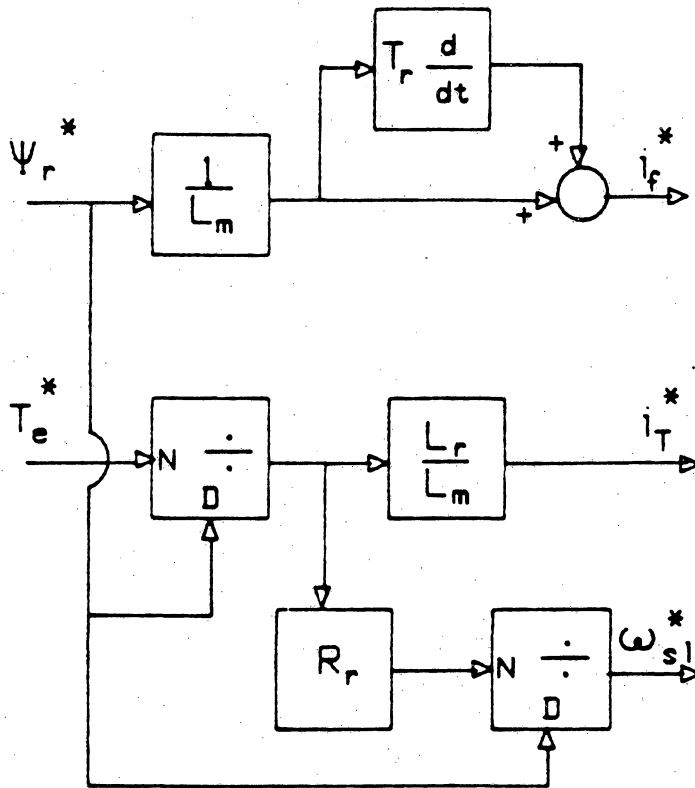


Figure 6. Schematic of Indirect Vector Controller.: N : numerator, D : denominator

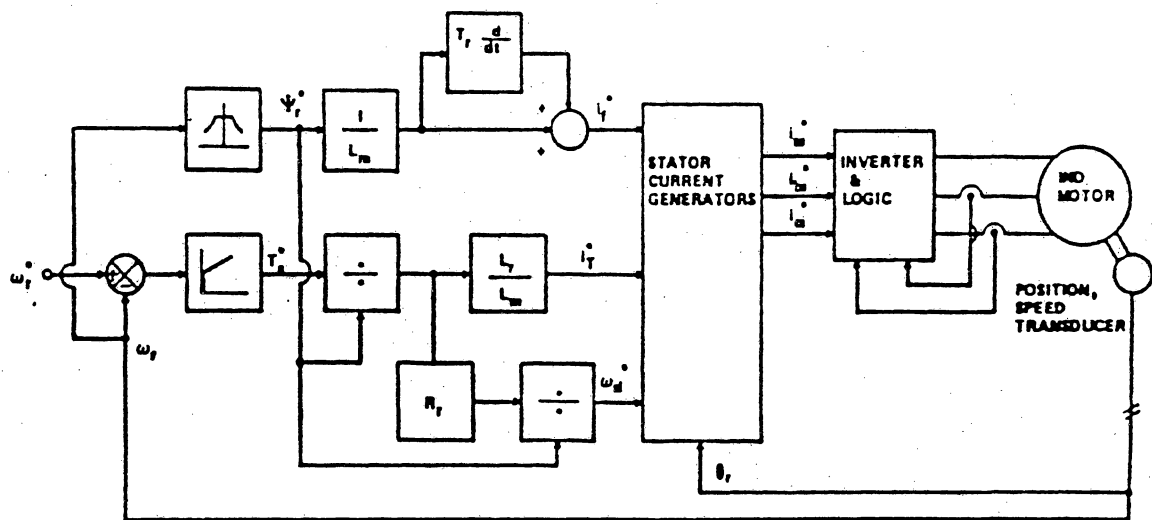


Figure 7. The indirect vector controlled drive system

ceeds to analyze the transient and steady state behavior of the induction motor drive system.

3.0 MODELING OF VECTOR CONTROLLED INDUCTION MOTOR

3.1 Introduction

The vector controlled induction motor drive consists of the induction motor, vector controller, inverter and the current and speed controllers. The models of these sub-systems are presented in this chapter. The dynamic model of the entire drive system is obtained by integrating the models of these sub-systems.

3.2 Model of the induction motor

The induction motor of the vector controlled drive system is fed from an inverter. The instantaneous effects of varying voltages/currents, stator frequency should be considered in the model. Hence the dynamic d-q axis model of the induction motor in synchronously rotating frame is used. The detailed derivation of the model is given in reference [10].

3.3 Model of the inverter

The inverter circuit used in the drive system is shown in Fig.8.

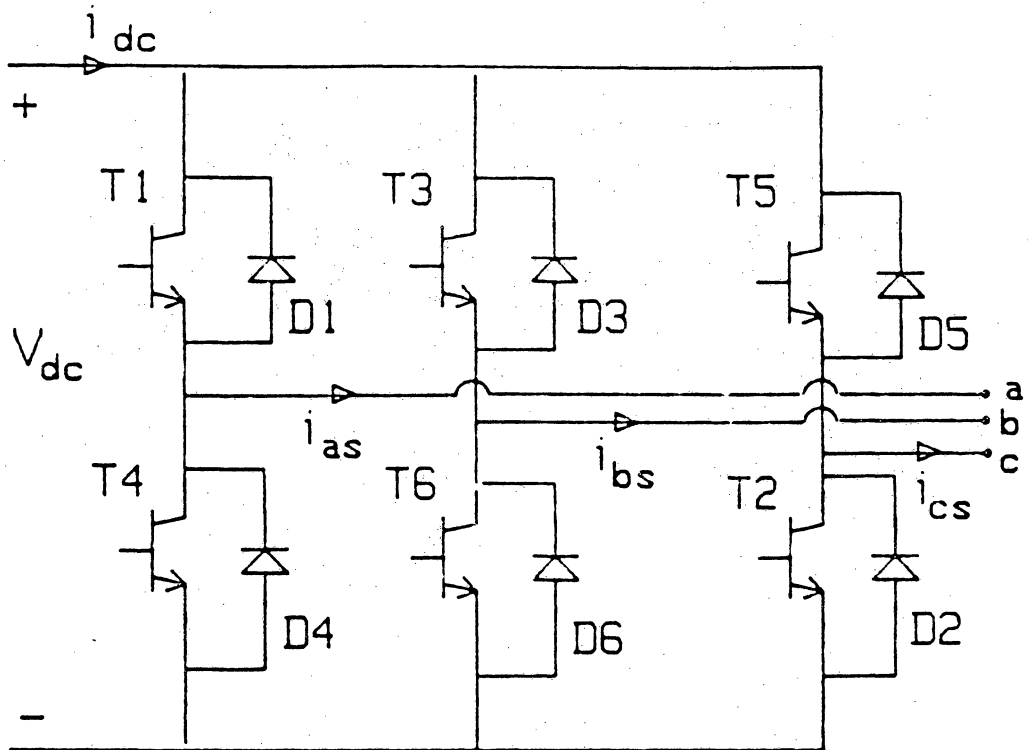


Figure 8. The inverter circuit

A constant dc voltage is assumed to be available to the inverter input. The six switches T_1 to T_6 are used to control the three-phase stator currents of the motor. The switches can be controlled using a hysteresis type current controller or a PWM type of current controller. A brief description of the two types of controllers is given below.

3.3.1 Hysteresis Current Controller

The actual currents flowing in the a and b phases of the stator are measured. The third current is calculated from the values of the other two phase currents. This eliminates the need for the third current sensor. The comparison between the commanded currents and the actual currents is done as shown in Fig.9. The objective of the controller is to maintain the actual current within $i_a^* + \Delta i$ and $i_a^* - \Delta i$. The middle curve in Fig.9. corresponds to the commanded current i_a^* . The upper curve and lower curves correspond to $i_a^* + \Delta i$ and $i_a^* - \Delta i$ respectively. The switching logic is given below in Table 1.

Table 1.

i_a^*	i_a	T_1	T_4	V_{an}
≥ 0	$i_a \leq (i_a^* - \Delta i)$	ON	OFF	$+V_{dc}/2$
≥ 0	$i_a \geq (i_a^* + \Delta i)$	OFF	OFF	$-V_{dc}/2$
< 0	$i_a \geq (i_a^* + \Delta i)$	OFF	ON	$-V_{dc}/2$
< 0	$i_a \leq (i_a^* - \Delta i)$	OFF	OFF	$+V_{dc}/2$

Switching Logic of the Hysterisis current controller

Whenever T_1 is 'on', i_a increases positively using either the B or C phases as a return path. When T_1 is switched from 'on' position to 'off' position and since the current through the machine winding cannot go to zero instantaneously, the freewheeling diode

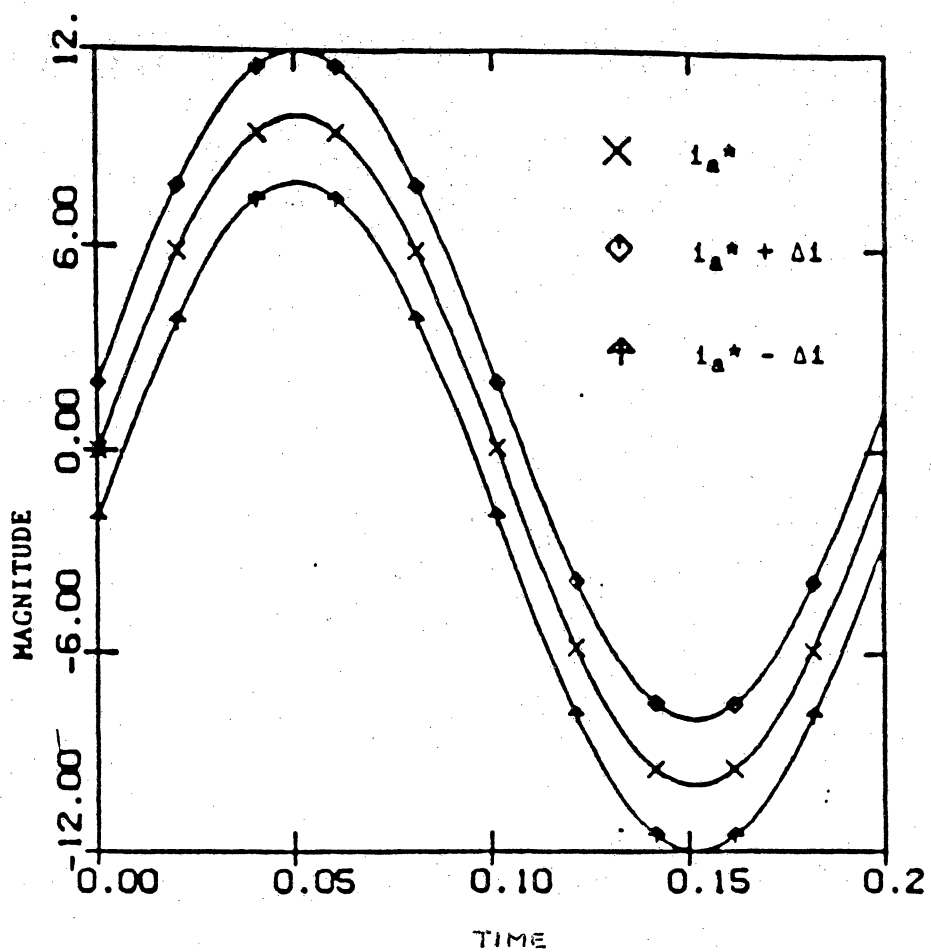


Figure 9. Comparison of commanded and actual currents

across the complimentary transistor, T_4 in this case begins to conduct the phase current. If the midpoint of the dc supply V_{dc} is taken as the reference then, voltage of phase A switches from $+V_{dc}/2$ to $-V_{dc}/2$ as a result of the above switching. The opposite occurs when T_1 switches from 'on' to 'off'. A similar logic applies to the other phases. Since the voltage is switched between positive and negative to maintain the phase currents within a band, this type of controller is called an hysteresis controller. The phase currents are therefore approximately sinusoidal. The smaller the hysteresis band the closer the actual current to the commanded current. It should be noted that the smaller the hysteresis band the higher the switching frequency of the inverter.

The control logic is used to model the hysteresis current controller. Each and every switching of the inverter power switches is simulated for accurate determination of the drive performance.

3.3.2 PWM Current Controller

In this method of current control, pulse width modulation technique is used to generate the actual stator currents. The actual and commanded currents are compared and the error signals are generated. The error signal is compared to a sawtooth shaped triangular wave as shown in Fig.10.

If the current error signal is smaller than the sawtooth, the voltage is switched negative, while if the error current is greater than the of the sawtooth, the voltage is switched positive. The phase voltage is pulse width modulated. The switching frequency of the inverter is preset in this method. It is thus easy to ensure that the inverter maximum frequency is not exceeded. A triangular sawtooth wave of 2kHz is used in the model of

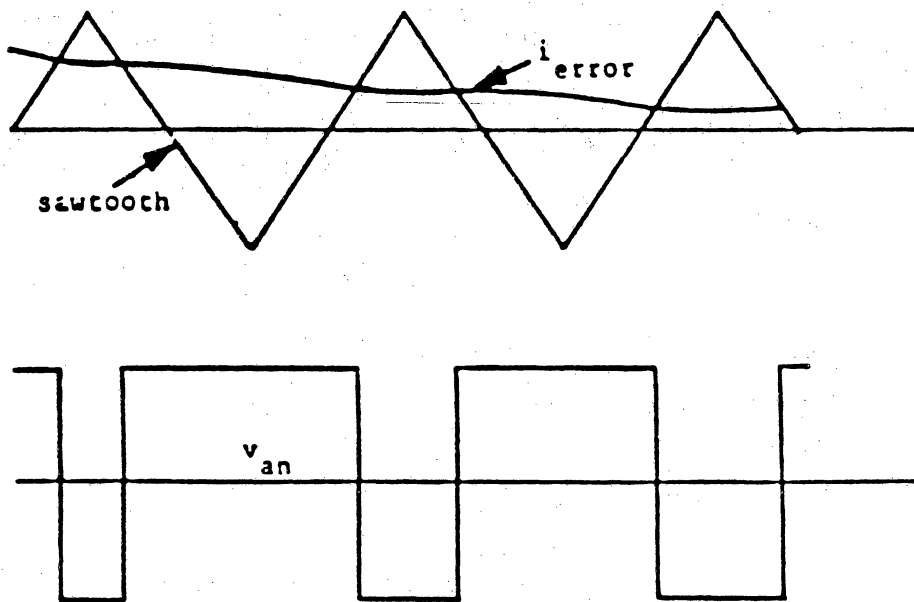


Figure 10. PWM controller switching logic

the PWM controller. The difference between the commanded value of current and the actual value of current is termed as error current.

Table 2.

PWM current controller's switching logic

(sawtooth voltage - error current)	V_a
positive	$-V_{dc}/2$
negative	$+V_{dc}/2$

A similar logic applies to the other phases also.

3.4 Model of the Vector Controller

The vector controller accepts the commanded values of the torque and flux to generate the command values for the torque producing component, the flux producing component of the stator current and the slip of the motor. The following equations model the indirect vector controller :

$$i_T^* = K_{it} \left[\frac{T_e^*}{\psi_r^*} \right] \left[\frac{L_r^*}{L_m^*} \right] \quad (3.1)$$

$$\text{Where } K_{it} = \frac{4}{3P}$$

$$i_f^* = \frac{1}{L_m^*} [1 + T_r^* p] \psi_r^* \quad (3.2)$$

$$\omega_{sl}^* = \left[\frac{L_m^*}{T_r^*} \right] \left[\frac{i_T^*}{\psi_r^*} \right] \quad (3.3)$$

These models of the motor, inverter and the indirect vector controller are integrated to give the dynamic model of the entire drive system. The simulation and analysis of the drive system are described in the next chapter.

3.5 The speed controller

A proportional plus integral type of speed controller is used in the speed drive system. The input to this controller is the speed error signal and torque command forms the output. The transfer function of this system is given below.

$$T_e^* \frac{(s)}{(\omega_r^*(s) - \omega_r(s))} = K_p + \frac{K_i}{s} \quad (3.4)$$

K_p and K_i are the proportional and integral gains respectively. The time domain equivalent of the equation is used to model the speed controller. The block diagram of the speed controller is shown in Fig.11.

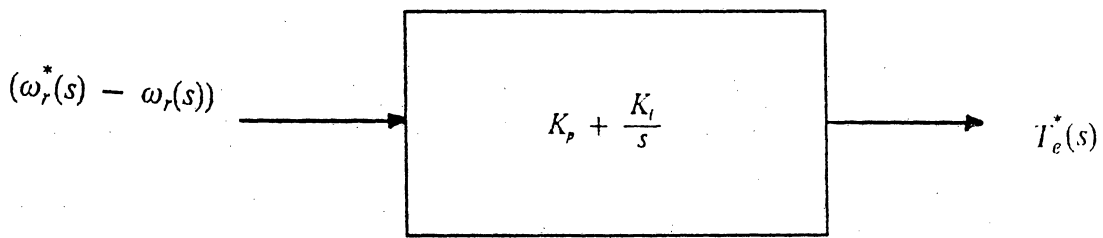


Figure 11. Block diagram of the speed controller.

4.0 SIMULATION AND ANALYSIS

4.1 Introduction

The indirect vector controlled induction motor drive system is a nonlinear multivariable control plant. The system may give rise to stability problems. The motor may interact dynamically with the source impedances of the converter/inverter. The inverter does not react instantaneously to the commanded signal. There is always a time lag between the command and its response. The developments in semiconductor power devices have reduced this delay, but it is not entirely eliminated. This delay may also compound the stability analysis of the system. The analytical study of this system is not possible and therefore computer simulation of the system becomes essential. The simulation is a valuable tool in the validation of the drive system design.

The torque drive (open speed-loop) system and the speed drive system are simulated and the results are analysed. For both the systems the induction motor parameters given in Appendix 2 were used.

4.2 Torque drive system

The vector controlled induction motor torque drive system accepts two inputs namely, the torque command and flux command. These signals are processed by the vector controller and the command values of stator currents are generated. The generation of

stator phase current commands requires the rotor position θ_r . A position transducer is used to get this value. The difference in the actual and commanded current is the error. The error signal forms the input to the current controller. The inverter firing logic is determined by the current controller. Thus the actual current is made to follow the commanded current. The torque drive system is shown shown in Fig.12.

The models of the induction motor and the vector controller described in the last chapter are used along with the inverter logic to simulate the torque drive system. The equations of the drive system are written in state variable form. There are 6 states in the torque drive system. They are i_{qs} , i_{qr} , i_{ds} , i_{dr} , ω_r , and θ_{sl} . The input vector consists of v_{qs} , v_{qr} , v_{ds} , and v_{dr} .

The state equations along with the vector controller equations and inverter logic form the model of the torque drive system. The time domain digital simulation of the drive system is achieved using FORTRAN. The fourth-order Range-Kutta method is used to solve the nonlinear state equations of the system. This method gives accurate results with less computation. A integration time step of 5 micro-seconds is used. The flow chart of the program to simulate the drive system is given in Fig.13.

The transistor switching delays are negelected in the simulation, but the program is flexible enough introduce them when the need arises. The saturation and iron-losses of the machine are neglected.

In a torque drive system the motor is started and brought to the desired speed before a torque is commanded. This ensures that the flux in the machine is at 1 pu value. The same condition is simulated by fixing the rotor speed at a desired value and giving a zero torque command. The flux will gradually build-up and reach the commanded flux value. The flux build-up is shown in Fig.14.

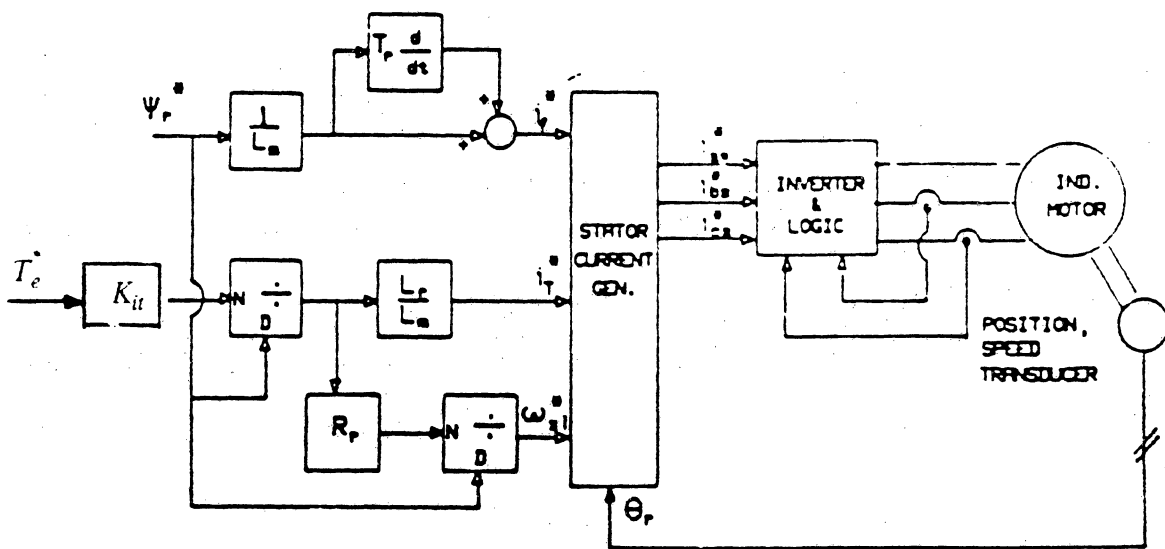


Figure 12. Torque drive system

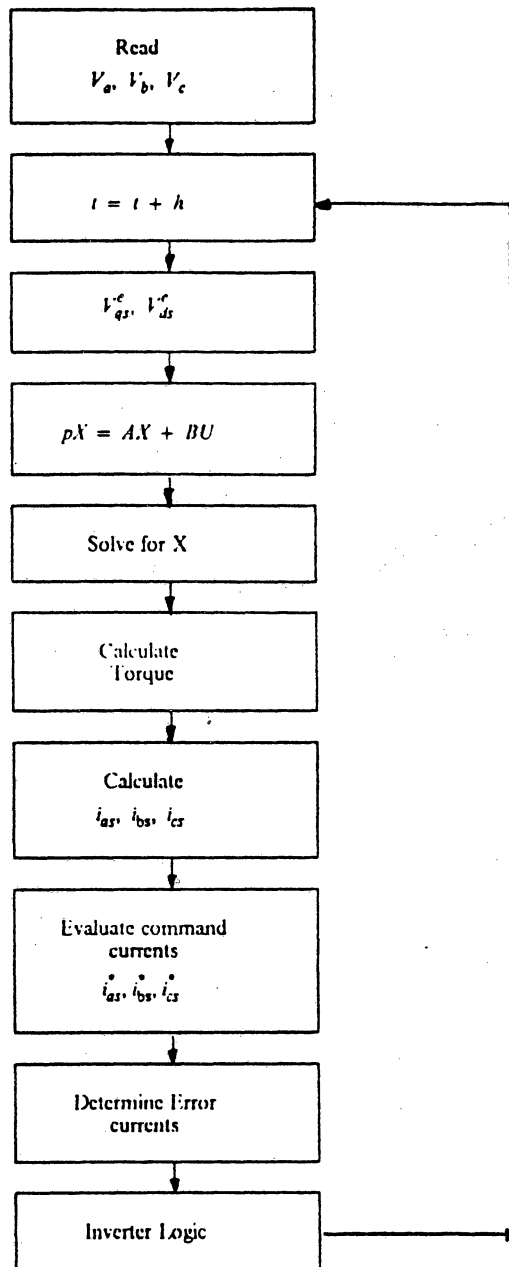


Figure 13. Flow chart to simulate the induction motor drive

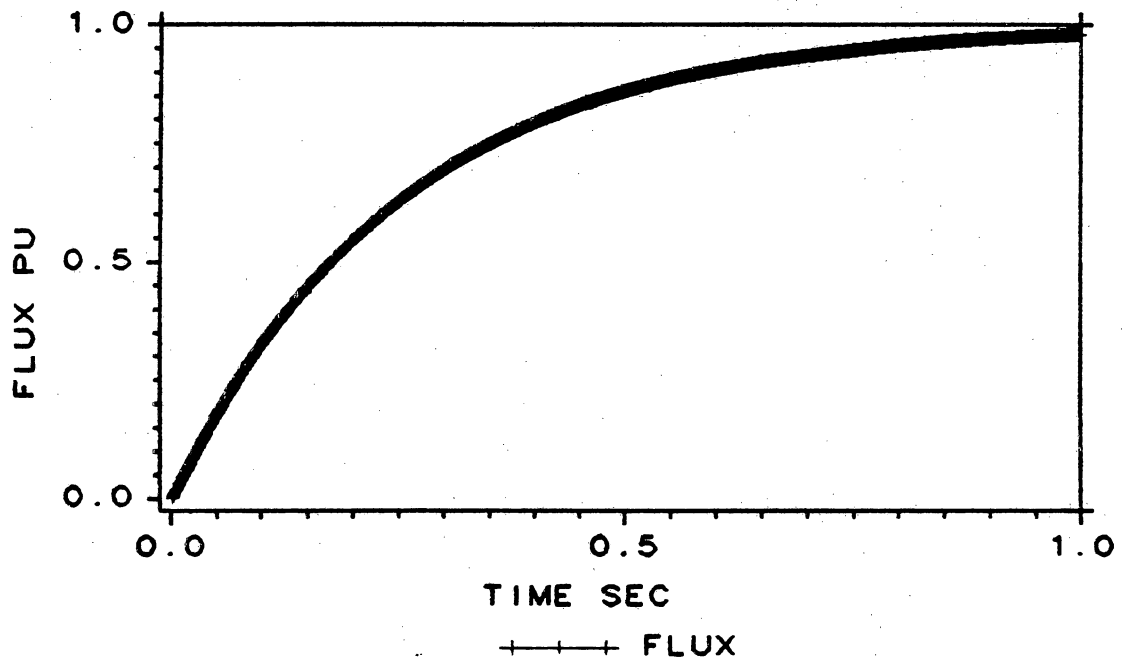


Figure 14. Building up of flux: Flux command is 1pu, torque command is 0pu

To analyze the performance of the torque drive system, the rotor speed has been fixed at 50 radians/second and a 1 pu value of flux was commanded. After the flux has reached 1 pu, a torque of 1 pu is commanded. At $t = 0.125$ seconds a torque command of -1pu was commanded. The response of the system to this type of torque command is shown in Fig.15. An hysteresis current controller was used in the above case.

The electric torque of the machine reaches the commanded value in a very short time. The 'a' phase current is also plotted and is shown in the same figure. The phase current increases to supply the commanded torque. The torque of the machine is seen to be pulsating. The pulsations are due to the switching of the inverter.

Similar procedure is used to get the response of the torque drive system with a PWM current controller. A PWM carrier frequency of 2 kHz is used. The responses of torque and current are similar and are shown in Fig.16.

4.2.1 Comparison between PWM and Hysteresis Current Controllers.

From the results of simulation of the torque drive system with hysteresis and PWM current controllers, the following conclusions are arrived at :

1. The torque pulsations are smaller with a PWM current controller than with a hysteresis controller.
2. The torque pulsations of a hysteresis current controller drive can be made smaller by decreasing the size of the hysteresis band.
3. The smaller the hysteresis band, the larger the switching frequency of the inverter.

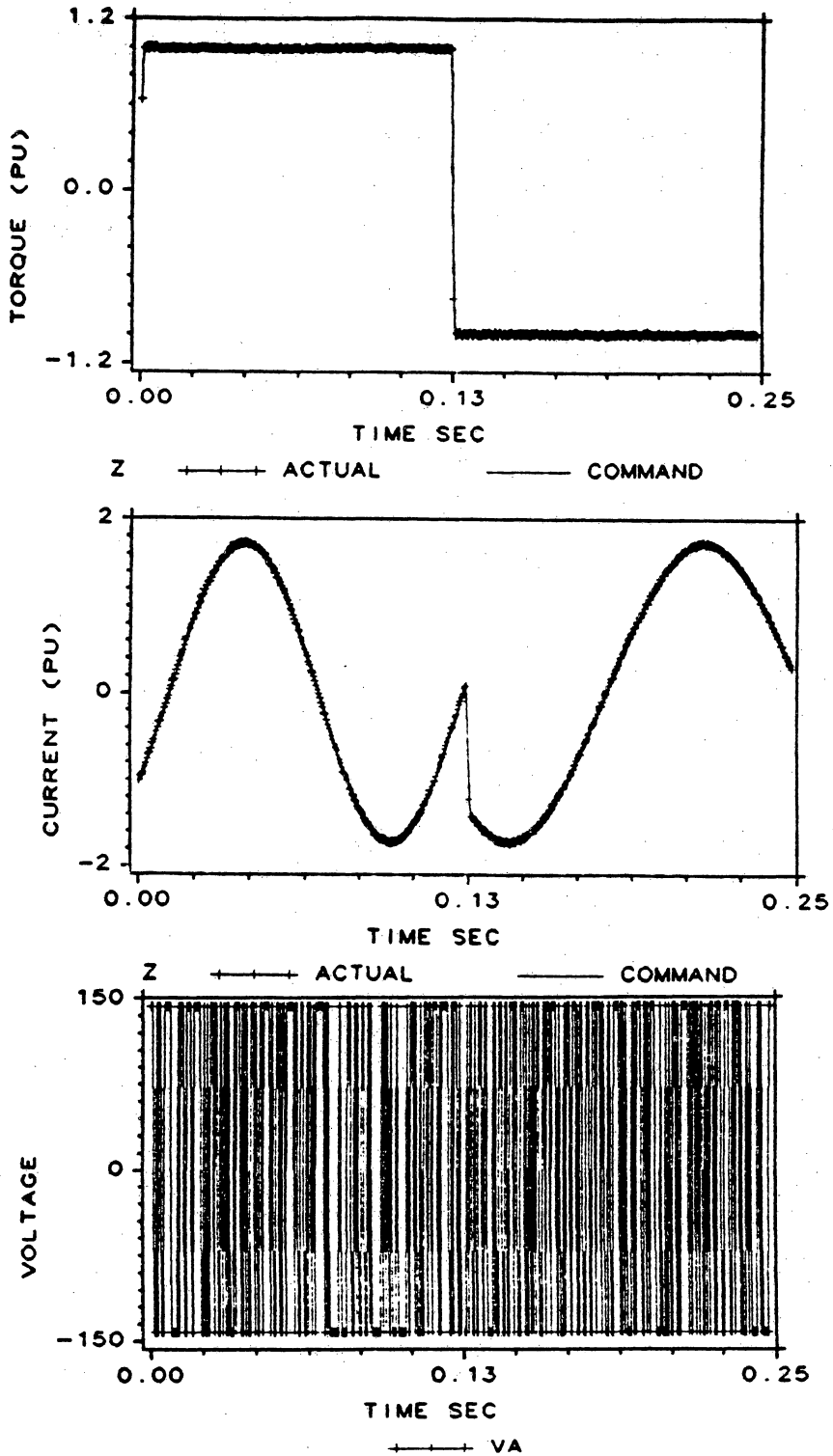


Figure 15. Response of the torque drive system with hysteresis controller: Current window size is 0.02A. Speed of the rotor is 240 rpm.

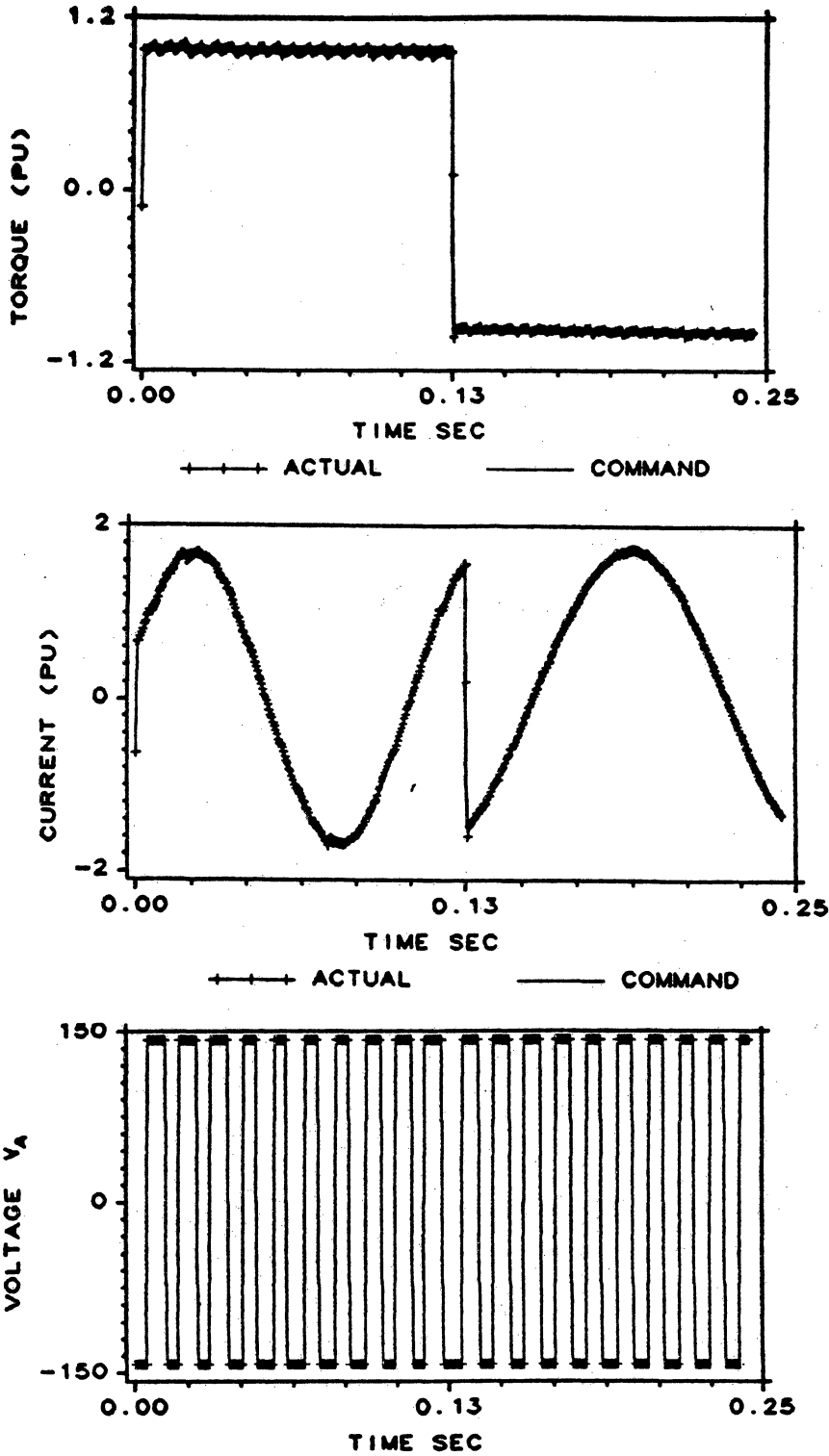


Figure 16. Response of the torque drive system with PWM controller: PWM frequency is 2kHz. Speed of the rotor is 240 rpm.

The variation of torque pulsations as function of the size of the current window is plotted is given in Fig.17.

In PWM type of current controller the switching frequency of the inverter is preset. Hence it is easy to design a controller in which the recommended switching frequency of the power devices is not exceeded. In a hysteresis current controller, the switching frequency of the power devices is not known. It is a function of the hysteresis band size. A trial and error method must be adopted to ensure that the recommended inverter switching frequency is not exceeded. The advantage of the hysteresis current controller over that of a PWM current controller is the absence of transportation delay or system lag. In a PWM controller this lag exists and the average value of this lag is equal to half the period of the PWM. If the lag is less than one tenth of the stator time constant, it has negligible effect on the system. Thus the PWM controller is more attractive than the hysteresis controller for the above application.

4.3 Speed drive system

The control block diagram of the speed drive system is shown in Fig.7. The speed of the motor is sensed and compared with the commanded speed. The difference in commanded and actual speed corresponds to the error signal. This error signal is passed through a speed controller. The speed controller is a proportional plus integral type of controller. The integral element is introduced to make the steady state error zero. The addition of the integral element makes the system response sluggish. Hence, the integral gain is kept small compared to the proportional gain.

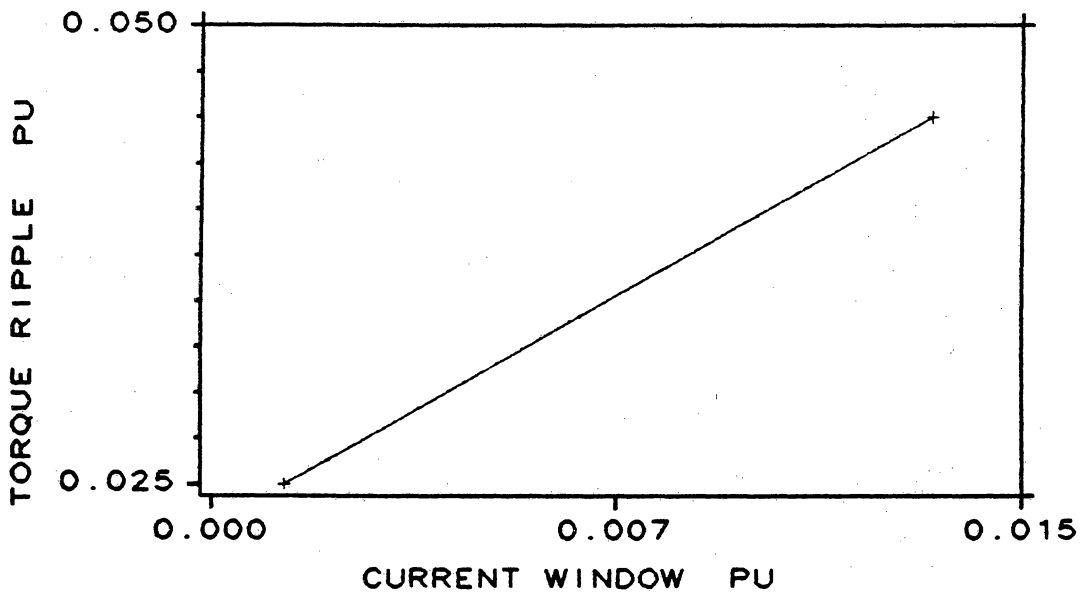


Figure 17. Variation of torque pulsations with current window size: Torque command is 1 pu, speed of the motor is 0.28 pu.

The simulation of the speed drive system is very similar to that of a torque drive system, except for the addition of one more state equation. The PI controller adds a new state to system. The output of the PI controller is limited to 2 pu. This limiting is essential because the induction motor's torque should not exceed 2 pu value. The performance of the speed drive system is predicted by simulation. The simulation is performed with a speed command of zero and a flux command of 1 pu. The flux in the machine increases gradually and reaches a steady state value of 1 pu. The state vector at this instant is used as the initial condition vector for the next simulation run. A speed command of 1 pu is given to system. After 0.25 seconds a load-torque of 1 pu is put on the machine. The responses of the system to this type of input is shown in Fig.18. for a hysteresis current controller and in Fig.19. for a PWM current controller.

The speed increases linearly and reaches the commanded speed. The application of load torque produces a very small dip in the speed. The vector control technique is responsible for the linear increase in speed of the machine. The drive is suited for high-performance applications because of its fast and precise response to commanded signal.

A more general way of testing the drive system is to observe its response to step changes in speed command. A speed of -1 pu is commanded at time $t = 0$. After 0.25 seconds a speed command of +1 pu is given to the system. The speed, torque and current responses to the above type of command are shown in Fig.20. and Fig.21.

The responses of the speed drive with hysteresis and PWM current controllers are similar. Once again it is seen that the torque ripple is high in the hysteresis current controlled drive. The stator currents follow the commanded currents in both the cases. The PWM controller appears to be more attractive for this case also.

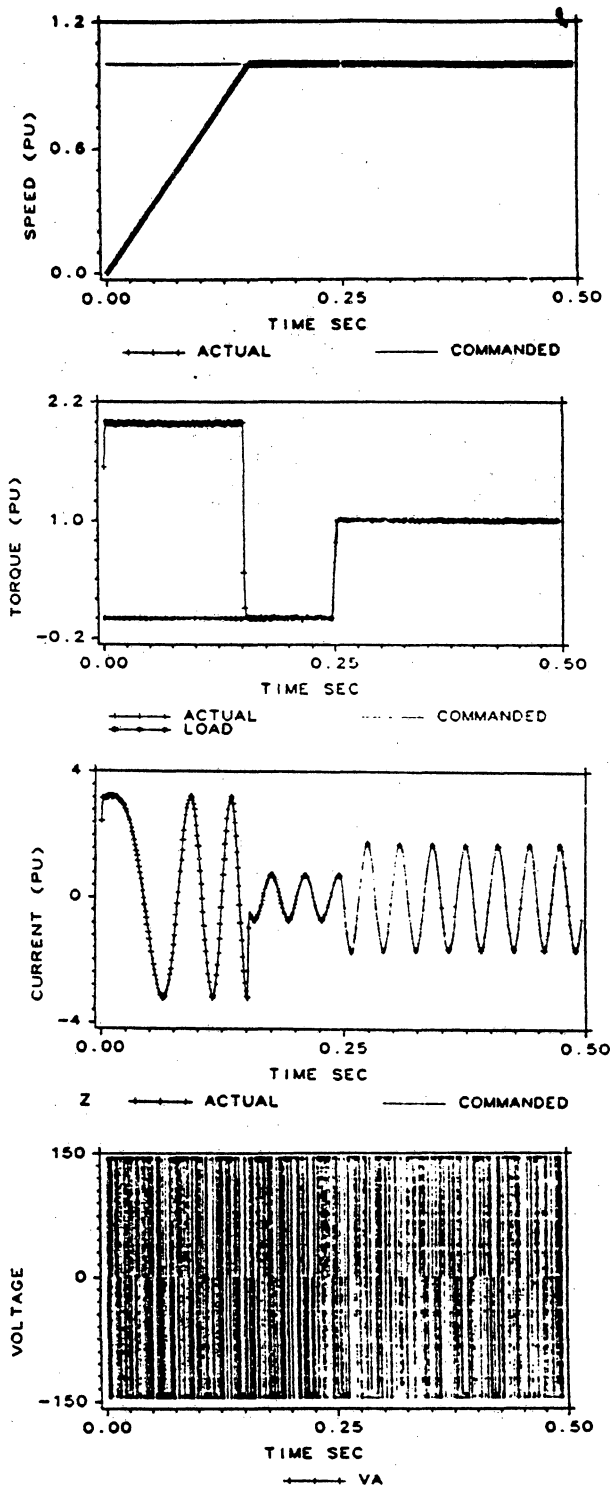


Figure 18. Response of the speed drive system with hysteresis controller: Current window size is 0.02A.

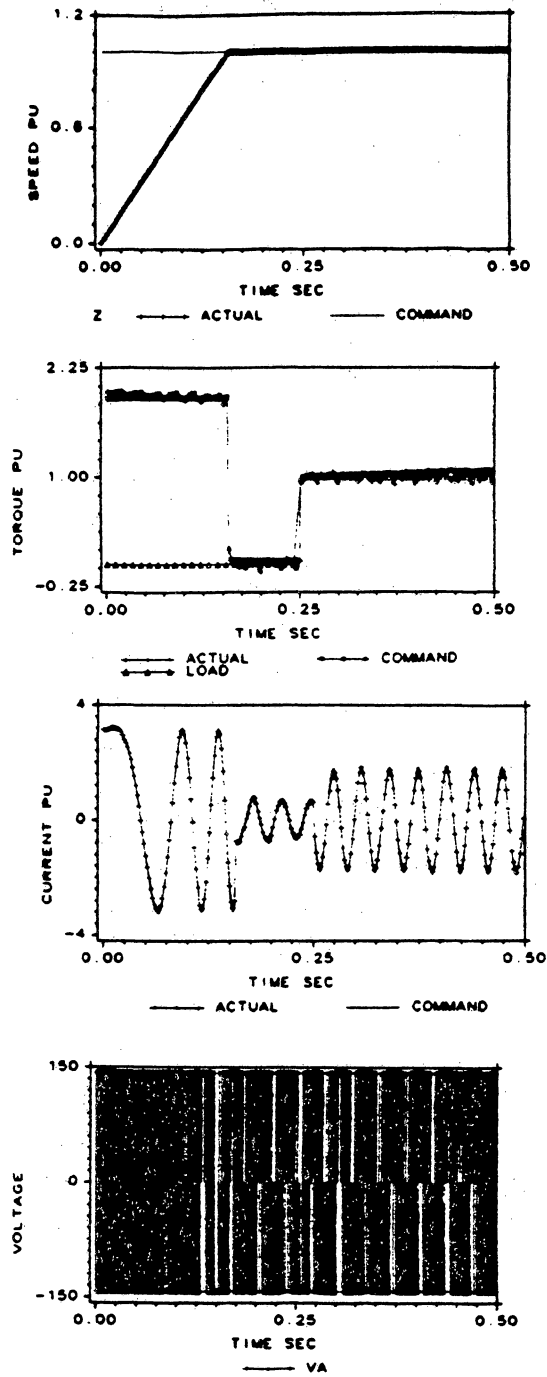


Figure 19. Response of a speed drive system with PWM control: PWM frequency is 2 kHz.

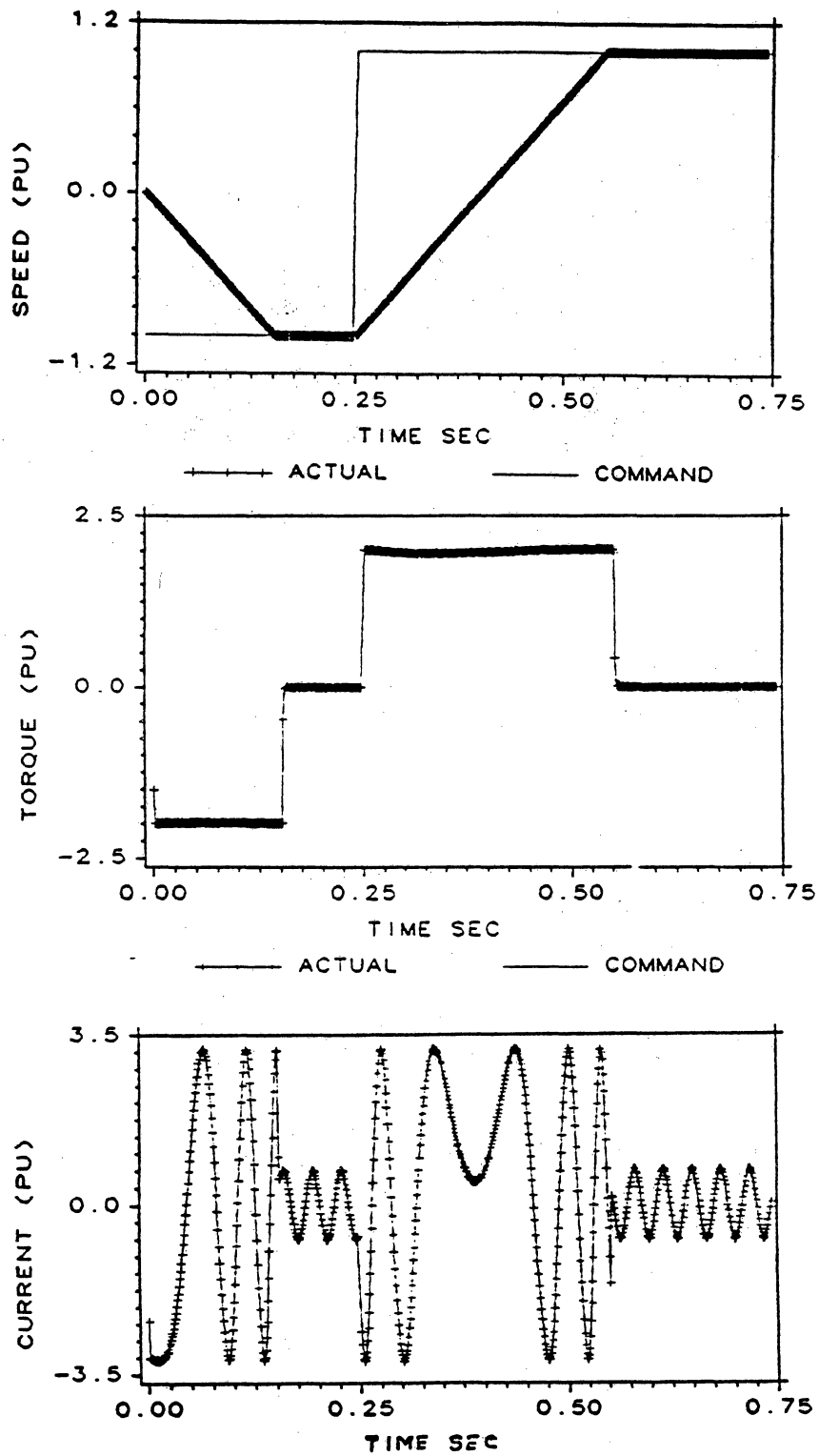


Figure 20. Response of the speed drive system with hysteresis control to a step input: Current window size is 0.02A, load torque is 0.0pu.

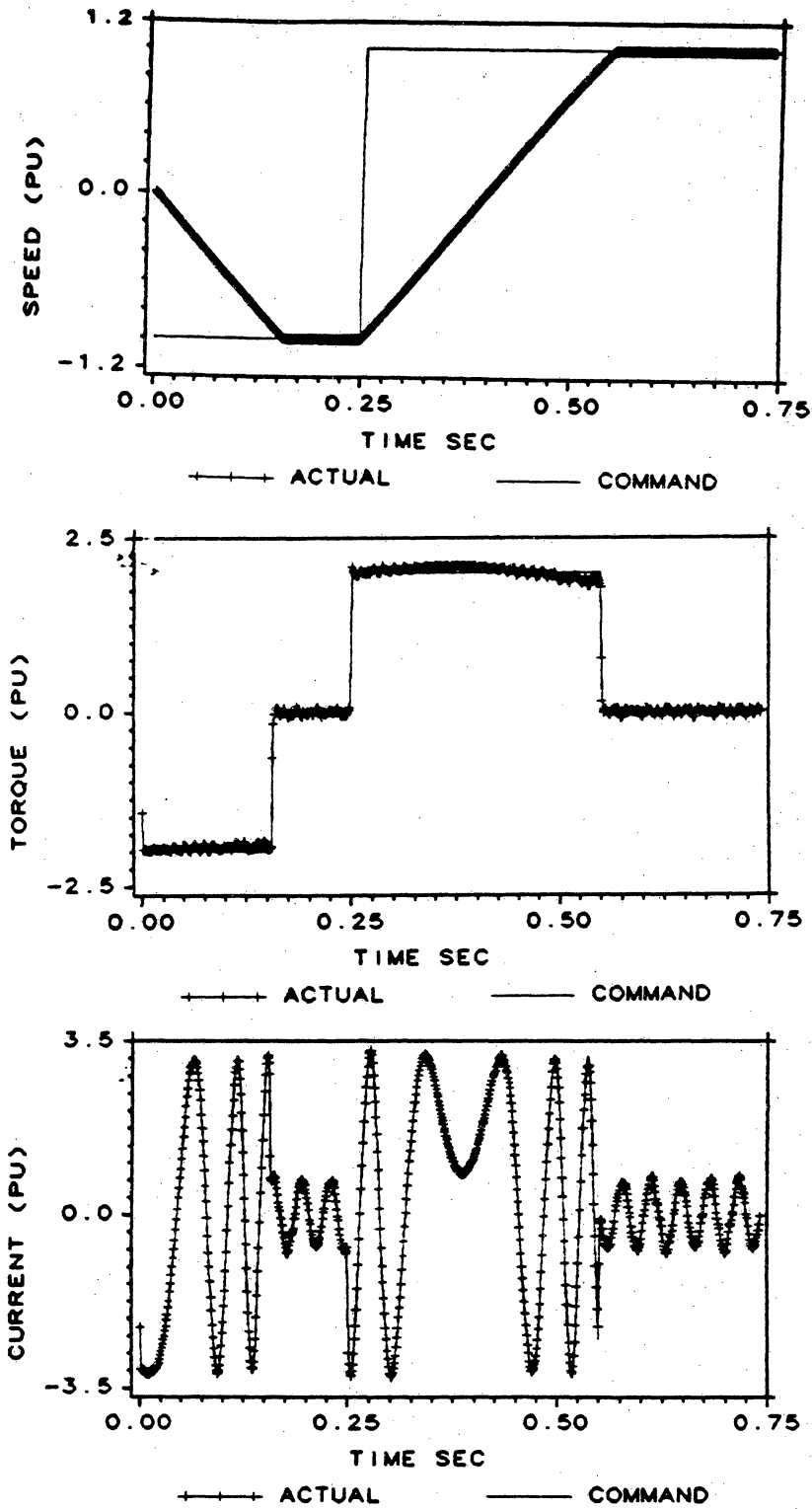


Figure 21. Response of the speed drive system with PWM controller to step input: PWM frequency is 2 kHz, load torque is 0.0p

5.0 SMALL SIGNAL FREQUENCY DOMAIN ANALYSIS

5.1 Introduction

The dynamic equations of the induction motor drive system have been derived in chapter 2 and chapter 3. These equations are nonlinear in nature as some of the terms are produced by the product of two current variables or a current variable and rotor speed. For the frequency domain study and the controller design it is necessary to linearise the dynamic equations around an operating point and use the powerful linear control techniques. The linear control techniques like the Bode plots, Nyquist plots and root locus can be used to determine the stability of the drive system. The poles, zeros and the gains of the transfer functions vary with the operating point. Hence the stability of the system for the worst operating conditions must be analyzed.

This chapter presents the linearisation of the system equations and the derivation of the necessary transfer functions of the drive system. Bode plots of the actual torque to commanded torque and actual speed to commanded speed transfer functions are given. The stability of the torque and speed drives and their bandwidths are discussed.

5.2 The small signal model

The nonlinear dynamic equations of the induction motor drive are linearised around an operating point using the perturbation technique. The linearised model is valid only for small signals or small disturbances. The induction motor model in synchronously rotating frame is used for perturbation because the steady state operating point consists of dc values. The linearised equations are obtained as follows :

The voltages, currents, torque, stator frequency and rotor speed are perturbed. The steady state value of these variables is designated by the subscript 'o'. The perturbed increments are designated with a δ preceding the variables. Accordingly the variables after perturbation are,

$$i_{qs}^e = i_{qso}^e + \delta i_{qs}^e \quad (5.1)$$

$$i_{ds}^e = i_{dso}^e + \delta i_{ds}^e \quad (5.2)$$

$$i_{qr}^e = i_{qro}^e + \delta i_{qr}^e \quad (5.3)$$

$$i_{dr}^e = i_{dro}^e + \delta i_{dr}^e \quad (5.4)$$

$$T_e = T_{e0} + \delta T_e \quad (5.5)$$

$$T_l = T_{l0} + \delta T_l \quad (5.6)$$

$$\omega_s = \omega_{s0} + \delta \omega_s \quad (5.7)$$

$$\omega_r = \omega_{r0} + \delta \omega_r \quad (5.8)$$

where

$$T_{eo} = \frac{3}{2} \frac{P}{2} L_m [i_{qso}^e i_{dro}^e - i_{dso}^e i_{qro}^e] \quad (5.9)$$

$$\delta T_e = \frac{3}{2} \frac{P}{2} L_m [i_{qso}^e \delta i_{dr} + i_{dro}^e \delta i_{qs}^e - i_{dso}^e \delta i_{qr}^e - i_{qro}^e \delta i_{ds}^e] \quad (5.10)$$

The stator currents are inputs to the drive system. The stator dynamics are neglected in the small signal frequency domain analysis. This assumption is valid because the stator currents follow the commanded values accurately because of the fast switching action of the inverter. This assumption means,

$$p i_{qs}^e = 0 \quad (5.11)$$

$$\text{and } p i_{ds}^e = 0 \quad (5.12)$$

The voltage balance equations of the rotor are

$$R_r i_{qr}^e + p \psi_{qr} + (\omega_e - \omega_r) \psi_{dr} = 0 \quad (5.13)$$

$$R_r i_{dr}^e + p \psi_{dr} - (\omega_e - \omega_r) \psi_{qr} = 0 \quad (5.14)$$

Substituting equations 5.1 - 5.10 in equations 5.13 and 5.14 and cancelling the steady state terms the small signal model of the induction motor drive is obtained. The equations are written in a state variable form as shown below.

$$pX = AX + BU \quad (5.15)$$

where

$$X = \begin{bmatrix} \delta i_{qr}^e \\ \delta i_{dr}^e \end{bmatrix} \quad (5.16)$$

$$U = \begin{bmatrix} \delta i_{qs}^e \\ \delta i_{ds}^e \\ \delta \omega_{sl} \end{bmatrix} \quad (5.17)$$

$$A = \begin{bmatrix} \frac{-R_r}{L_r} & -\omega_{slo} \\ \omega_{slo} & \frac{-R_r}{L_r} \end{bmatrix} \quad (5.18)$$

$$B = \begin{bmatrix} 0 & \frac{-L_m}{L_r} \omega_{slo} & \frac{1}{L_r} (L_m i_{dso} + L_r i_{dro}) \\ \frac{L_m}{L_r} \omega_{slo} & 0 & \frac{1}{L_r} (L_m i_{qso} + L_r i_{qro}) \end{bmatrix} \quad (5.19)$$

The output of interest is the torque, which is obtained as

$$y = CX + DU \quad (5.20)$$

where

$$C = \frac{3PL_m}{4} [-i_{dso} \quad i_{qso}] \quad (5.21)$$

and

$$D = \frac{3PL_m}{4} [i_{dro} \quad -i_{qro} \quad 0] \quad (5.22)$$

5.3 The frequency domain analysis of the torque drive system

The frequency domain analysis of the torque drive system is performed using the linearised small signal model developed in the previous section. The torque vs torque command and the flux vs flux command transfer functions are obtained to analyze the stability of the drive system.

To find the torque vs torque command transfer function, the inputs given by (5.17) are expressed in terms of T_e^* .

$$\delta i_{qs} = \frac{4L_r}{3PL_m\psi_r^*} \delta T_e^* \quad (5.23)$$

$$\delta i_{ds} = 0.0 \quad (5.24)$$

$$\delta \omega_{sl} = \frac{4R_r}{3P\psi_r^2} \delta T_e^* \quad (5.25)$$

The operating point is found from the simulation of the torque drive system. The Bode plot of transfer function between the actual and commanded torques is shown in Fig.22. The upper plot of Fig.22. obtained with an hysteresis current controller and the lower one is obtained with a PWM current controller. From the plots it is clear that the system is stable.

The transfer function obtained is verified as follows : The torque command is perturbed by 0.1pu. The response of the system to this small disturbance is simulated and also mathematically evaluated using the Laplace inverse transformation. The results of both

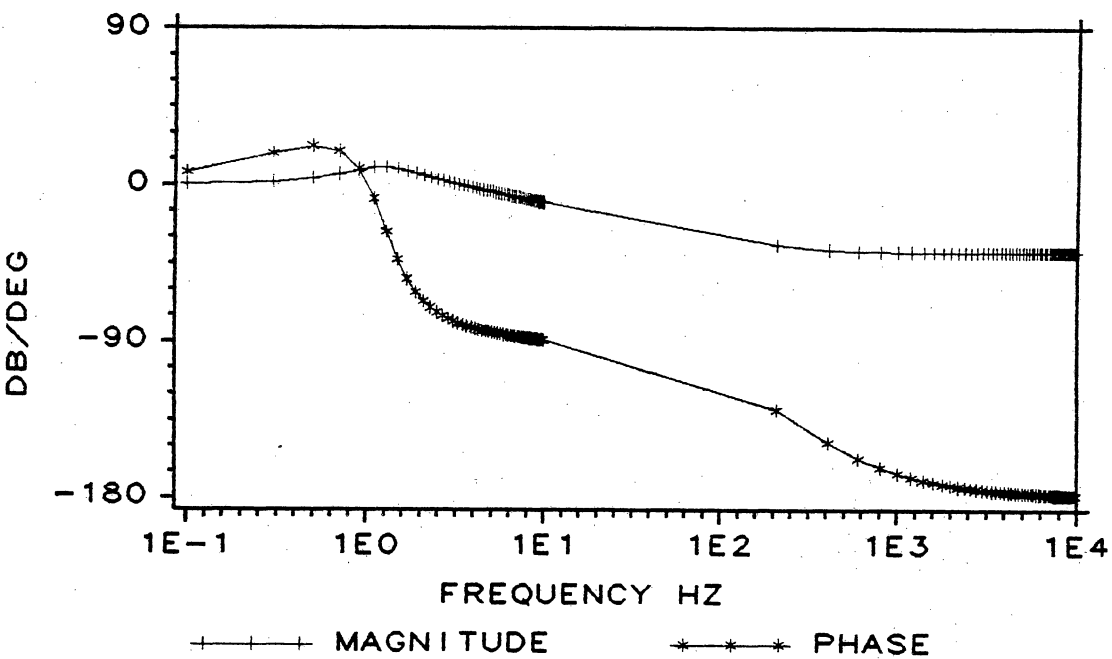
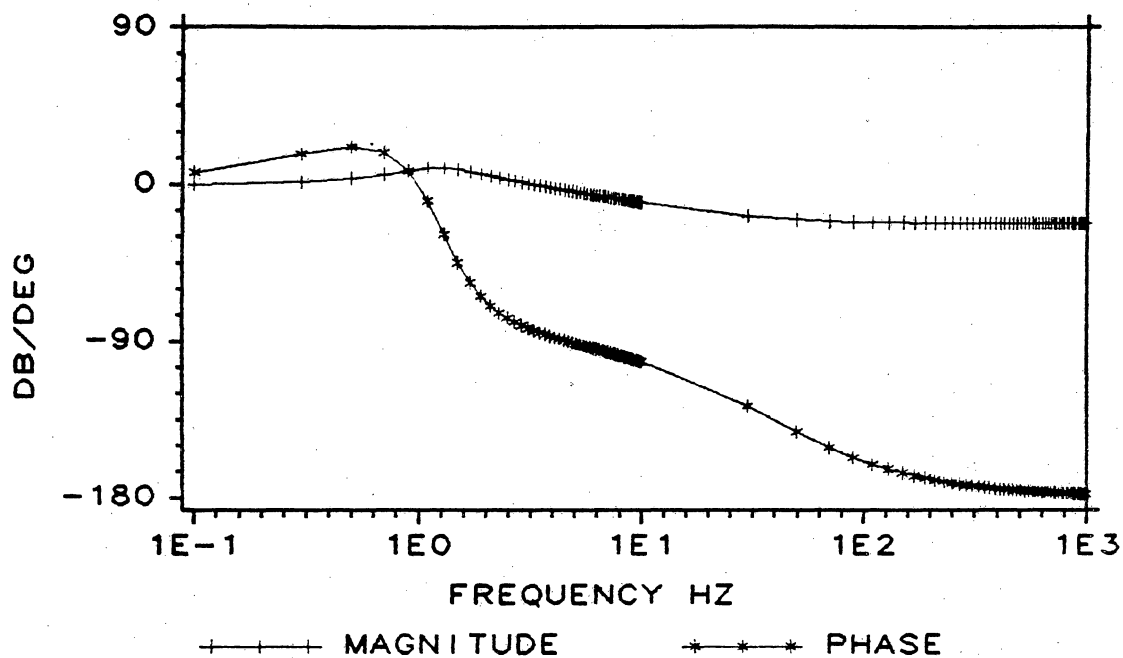


Figure 22. Bode plot of actual torque to commanded torque transfer function: 1pu torque at 0.26pu speed, Top : Hysteresis, Bot : PWM control

are plotted on the same graph and are shown in Fig.23. The results obtained by both methods tally very well, indicating that the transfer function obtained is correct.

The $\frac{\psi_r}{\psi_r^*}$ transfer function is obtained from the state model by writing the inputs in terms of $\delta\psi_r^*$.

$$\delta i_{qs}^* = -K_{it} T_e^* \frac{L_r}{L_m} \delta \psi_r^* \quad (5.26)$$

$$\delta i_{ds}^* = \delta \psi_r^* \quad (5.27)$$

$$\delta \omega_{sl}^* = -2K_{it} R_r \frac{T_e^*}{\psi_{ro}^*} \delta \psi_r^* \quad (5.28)$$

The output equation can be written as follows :

$$y = [0 \ L_r] X + [0 \ L_m \ 0] U \quad (5.29)$$

The Bode plot of this transfer function is shown in Fig.24. The upper plot is obtained from a system with an hysteresis current controller and the lower one is obtained with a PWM current controller.

5.4 The frequency domain analysis of the speed drive system

The speed drive system is obtained from the torque drive system by closing the speed loop. This involves sensing the actual speed and comparing it with the commanded speed. The error signal is sent through the speed controller. The speed controller is a proportional plus integral controller. The proportional gain is kept high while the inte-

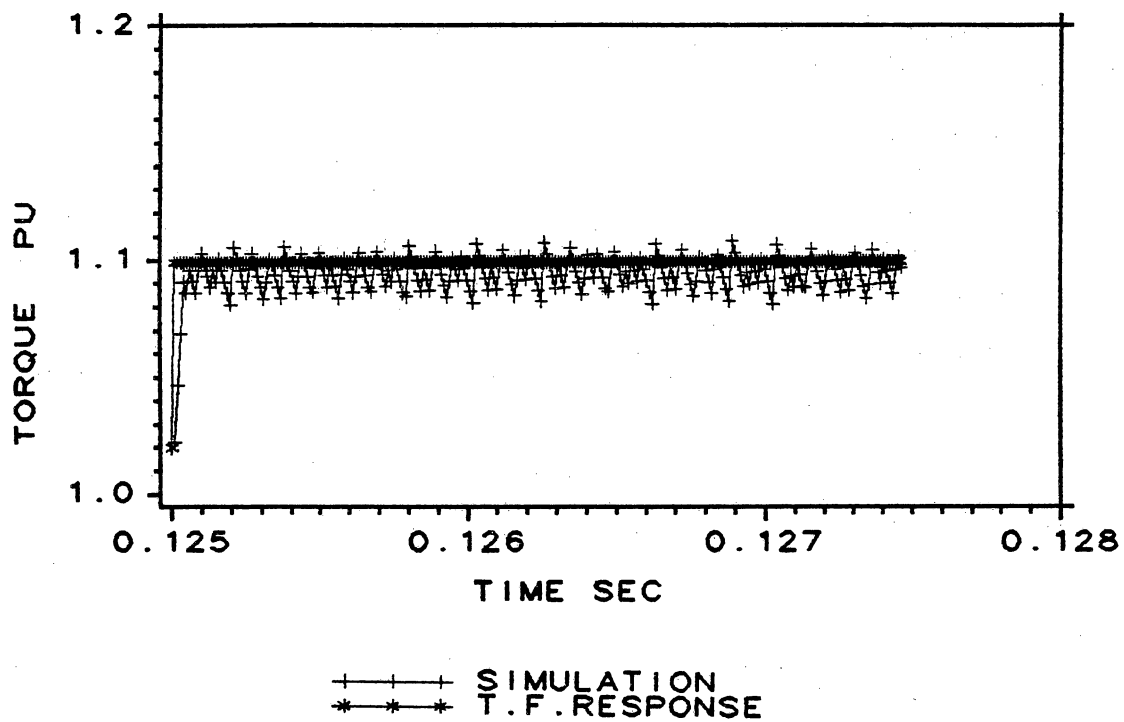


Figure 23. Transient response of the Torque drive system to a step input: 1.1pu torque at 0.26pu speed, step change is 0.1pu

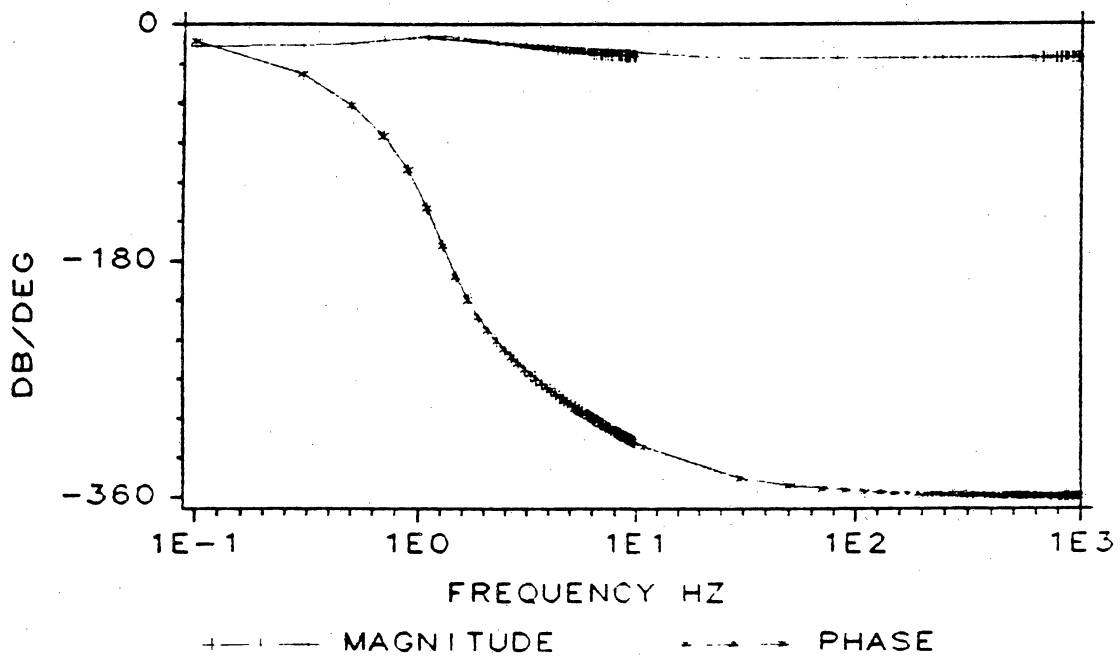
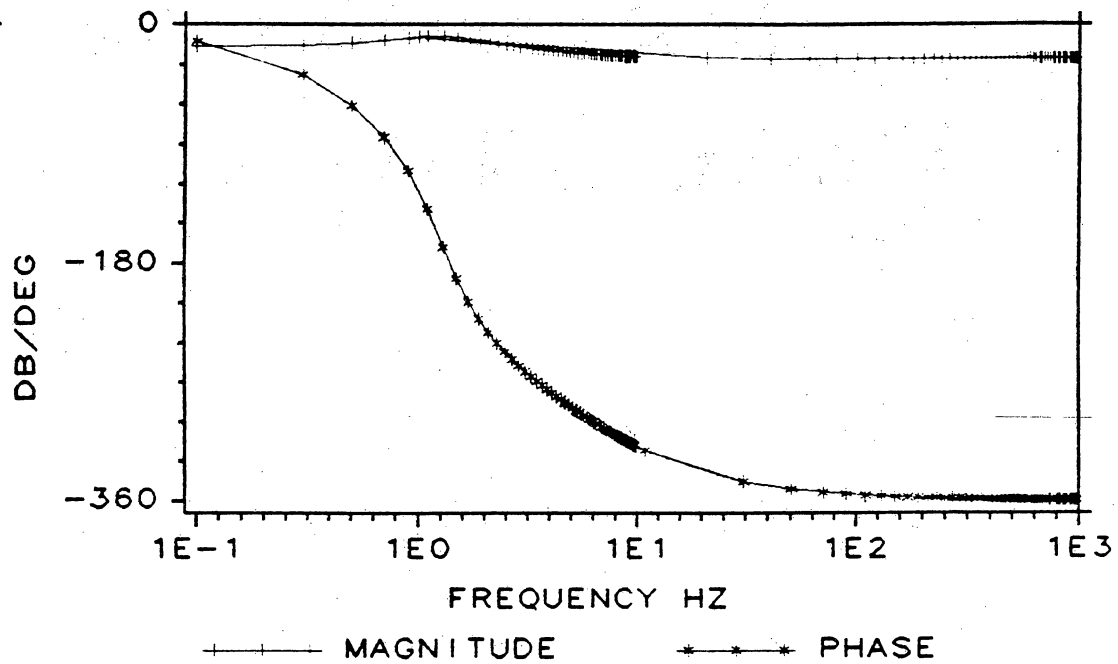


Figure 24. Bode plot of actual flux to commanded flux transfer function: 1pu torque at 0.26pu speed,
 Top : Hysteresis, Bot : PWM control

gral gain is kept small. The introduction of the controller increases the order of the system by one. The controller equation is perturbed and the small signal version of it obtained.

$$p\delta T_e^* = K_i(\delta\omega_r^* - \delta\omega_r) - K_p p\delta\omega_r \quad (5.30)$$

The mechanical equation for torque is

$$p\omega_r = \frac{P}{2J}(T_e - T_l) \quad (5.31)$$

These two equations along with the other small signal model equations give the small signal model of the speed drive system. The system can be represented as

$$pX = AX + BU \quad (5.33)$$

$$y = CX \quad (5.34)$$

where

$$A = \begin{bmatrix} \frac{-R_r}{L_r} & -\omega_{slo} & 0 & 0 \\ \omega_{slo} & \frac{-R_r}{L_r} & 0 & 0 \\ -\frac{3L_m P^2}{8J} i_{dso} & \frac{3L_m P^2}{8J} i_{qso} & 0 & 0 \\ 3P^2 L_m K_p \frac{i_{dso}}{8J} & -3P^2 L_m K_p \frac{i_{qso}}{8J} & -K_i & 0 \end{bmatrix} \quad (5.35)$$

$$B = \begin{bmatrix} 0 & -L_m \frac{\omega_{slo}}{L_r} & \frac{-1}{L_r}(i_{dso}L_m + L_r i_{dro}) & 0 & 0 \\ L_m \frac{\omega_{slo}}{L_r} & 0 & \frac{1}{L_r}(L_m i_{qso} + L_r i_{qro}) & 0 & 0 \\ 3L_m \frac{P^2}{8} i_{dro} & -3L_m \frac{P^2}{8} i_{qro} & 0 & \frac{-P}{2J} & 0 \\ 0 & 0 & 0 & 0 & K_i \end{bmatrix} \quad (5.36)$$

$$C = [0 \ 0 \ 1 \ 0] \quad (5.37)$$

$$X = [\delta i_{qr} \ \delta i_{dr} \ \delta \omega_r \ \delta T_e^*]^T \quad (5.38)$$

$$U = [\delta i_{qs} \ \delta i_{ds} \ \delta \omega_{sl} \ \delta T_l \ \delta \omega_r^*]^T \quad (5.39)$$

The operating point is again found from the simulation. The speed vs speed command transfer function is derived using the equations (5.33) - (5.39). The δi_{qs} , δi_{ds} and $\delta \omega_{sl}$ are written as functions of δT_e and the A matrix is modified to find the speed vs speed command transfer function.

5.4.1 The selection of speed controller gains

The speed controller is a proportional plus integral controller. The response of the system is controlled by the speed controller. The rise time and stability of the system are the important factors depend on the constants of the controller. The actual design of the controller is complicated and is not attempted. A trial and error method is used to select the gains of the controller. The integral term of the controller makes the response of the system sluggish, but it eliminates the steady state error. Hence the integral gain is kept small and the proportional gain is chosen to be large.

The simulation of the drive system is a valuable tool to analyze the time domain response of the system. The controller gains were selected to give a fastest possible response with no or very little over-shoot.

Table 3

Speed	Eigenvalues			
1pu	-0.005	-0.32	$-3.1 + j241.5$	$-3.1 - j241.5$
0.5pu	-0.0016	-3.34	$-1.6 + j151.5$	$-1.6 - j151.5$
0.25pu	-0.0006	-3.33	$-1.6 + j 235.7$	$-1.6 - j235.7$

Eigenvalues of the speed drive system for 3 operating speeds

The speed drive system is simulated for various values of commanded speeds. The eigen-values of the system are found for each operating point. A table of the eigen-values is given in Table 3 for the speed drive system with hysteresis current control. Similar values obtained for the speed drive system with PWM current control. The system is found to be stable for all the above operating points.

6.0 CONCLUSIONS

The objectives of this thesis were to model, simulate and analyze the indirect vector controlled induction motor drive.

The complexity of control of the induction motors was shown to be the major disadvantage for their use servo applications. The vector control transforms the induction motor control to an equivalent separately excited dc motor control. The dynamic modeling of the induction motor was presented. The vector controller equations were derived and used along with the induction motor equations to model the entire drive system. The real time models of the inverter and current controller were developed.

The torque drive system and speed drive system were simulated. The responses of these systems were analyzed. The behaviour of the system with hysteresis and PWM current controllers was studied. The PWM current controller makes the inverter switch at a constant frequency. It also produces a smaller torque ripple than the hysteresis controller. Faster response to command signals is achieved in the hysteresis type of current control.

The model of the drive system was linearised around an operating point and small signal frequency domain analysis was performed. The $\frac{T_e}{T_e^*}$, $\frac{\psi_r}{\psi_r^*}$ and $\frac{\omega_r}{\omega_r^*}$ transfer functions of the system were derived. The drive system was simulated for various values of the commanded speed and torque. The eigenvalues of the system for these operating points were obtained and the stability of the system was analysed.

6.1 Contributions

1. The models for the hysteresis and PWM current controllers were developed.
2. The models of the various sub-systems were integrated to form the dynamic model of the drive system.
3. Digital simulation of the entire drive system was performed using the above model.
4. Results of the simulation were analysed.

6.2 Scope for future work

The next logical step is to close the position loop of the drive system and study its behaviour. The vector controlled induction motor drive system can be implemented and the actual results can be compared with the simulation results.

Bibliography

- [1] F. Blaschke, "Das Verfahren der Feldorientierung zur Regelung der Asynchronmaschine", Siemens Forsch -u. Entwickl. - Ber.Bd.1,Nr.1, pp.184-193,1972 (In German)
- [2] T. Iwakane, H. Inokuchi, T. Kai and J. Hirai, "AC Servo Motor Drive for Precise Positioning Control", Conf. Record, IPEC, Tokyo, March 1983, pp. 1453-1464.
- [3] K. Kubo, M. Watanabe, T. Ohmae and H. Kamiyama, "A software-based speed regulator for motor drives", Conf. Record, IPEC, Tokyo, March 1983, pp. 1500-1511.
- [4] T. A. Lipo and A. B. Plunkett, "A new approach to induction motor transfer functions", Conf. Record, IEEE-IAS Annual Meeting, Oct. 1973, pp. 1410-1418.
- [5] R. Krishnan, J. F. Lindsay and V. R. Stefanovic, "Control characteristics of inverter-fed induction motor", IEEE transactions on Industry Applications, Vol IA -19, No.1, Jan/Feb 1983, pp. 94-104.
- [6] Myung J. Youn and Richard G. Hoft, "Variable frequency induction motor Bode diagrams", IEEE-IAS, ISPC Conference Record, 1977, pp. 124-136.
- [7] R. H. Nelson, T. A. Lipo and P. C. Krause "Stability analysis of a symmetrical induction machine", IEEE Transactions on Power Apparatus and Systems, Vol PAS - 88, No.11, Nov 1969, pp. 1710 - 1717
- [8] V. R. Stefanovic and T. H. Barton, "The speed - torque transfer function of electric drives", IEEE Transactions on Industry Applications, Vol. IA - B No.5, Sept/Oct 1977, pp. 428 - 436
- [9] R. Krishnan and P. Pillay, "Sensitivity analysis and comparison of parameter compensation schemes in vector controlled induction motor drives", Conf. Record, IEEE-IAS Annual Meeting, Oct. 1986, pp. 155-161.
- [10] R. Krishnan "Analysis of electronically controlled motor drives", Class Notes, VPI&SU, 1986.
- [11] James Singer, "Elements of numerical analysis", Academic Press, 1968.
- [12] D. M. Brod and D. W. Novotny, "Current control of VSI-PWM inverters", Conf. Record, IEEE-IAS Annual Meeting, Oct. 1984, pp. 418-425.

- [13] D. Dalal and R. Krishnan, "*Parameter Compensation of Indirect Vector Controlled Induction Motor Drive Using Estimated Airgap Power*", Conference Record, IEEE Industrial Applications Society annual meeting, Atlanta, pp. 170-176, Oct 1987.
- [14] R. Krishnan and Frank C. Doran, "*Study of Parameter Sensitivity in High-Performance Inverter-fed Induction Motor Drive*", IEEE Transactions on Industry Applications, Vol 1A-23, No 4., pp 623-635, July/Aug 1987.
- [15] R. Krishnan and Frank C. Doran, "*A Method of sensing line Voltages for Parameter Adaptation of Inverter-fed Induction Motor Servo Drives*", IEEE Transactions on Industry Applications, Vol 1A-23, No. 4, pp 617-622, July/Aug 1987.
- [16] R. Krishnan and Frank C. Doran "*Identification of Thermally Safe Load Cycles for An Induction Motor Position Servo*", IEEE Transactions on Industry Applications, Vol 1A-23, No.4, pp 636-642, July/Aug 1987.
- [17] R. Krishnan "*Selection Criteria for Servo Motor Drives,*" , IEEE Transactions on Industry Applications, Vol 1A-23 No.2, pp 270-275, Mar/Apr 1987.
- [18] J. F. Lindsay and M. H. Rashid, "*Electromechanics and Electrical machinery*" , Prentice - Hall Inc., Englewood Cliffs, N.J., 1986.
- [19] Paul C. Krause, "*Analysis of electric machinery*", Mc Graw-Hill Book Company, 1986.

Appendix A. Induction Motor Parameters

5 hp, Y-connected, 3 phase, 60 Hz, 4 pole, 200 V.

$$R_s = 0.277 \Omega$$

$$R_r = 0.183 \Omega$$

$$L_m = 0.05383 \text{ H}$$

$$L_s = 0.0553 \text{ H}$$

$$L_r = 0.05606 \text{ H}$$

$$J = 0.01667 \text{ Kg} \cdot \text{m}^2$$

Appendix B. List of symbols

All symbols marked with an asterisk indicate the commanded/reference value of the quantity.

ac, AC	Alternating current
B	Damping Factor
dc, DC	Direct current
E_r	Voltage Drop Across Effective Rotor Resistance
f_s	Synchronous Frequency (Hz.)
$i_{as} i_{bs} i_{cs} i_s^*$	Stator Phase Currents
i_a	Armature Current
i_f	Field (Flux Producing) Current
i_T	Torque Producing Current
i_{qs}^*, i_{ds}^*	d-q Axes Stator Currents
i_{qr}^*, i_{dr}^*	d-q Axes Rotor Currents
J	Moment of Inertia
K_f	Flux Constant
K_i	Integrator Gain
K_p	Proportional Gain
K_t	Torque Constant
L_{lr}	Rotor Leakage Inductance
L_{ls}	Stator Leakage Inductance
L_m	Mutual Inductance

L_r	Rotor Self Inductance
L_s	Stator Self Inductance
p	Differential Operator
P	Number of Poles
R_r	Rotor Resistance per Phase
R_s	Stator Resistance per Phase
s	Slip
T_e	Electrical Torque
T_L	Load Torque
T_r	Rotor Time Constant
$V_{s^*}, v_{as} v_{bs} v_{cs}$	Stator Phase Voltages
X_{lr}	Rotor Leakage Inductance
X_{ls}	Stator Leakage Inductance
X_m	Mutual Inductance
Δ_i	Hysteresis Current Window
θ_f	Field Angle (Flux Position Angle)
θ_r	Rotor Position Angle
θ_{sl}	Slip Angle
θ_T	Torque Angle
v_{ds}^e, v_{qs}^e	d-q Axes Stator Voltages
ϕ_f	Flux
ψ_{dr}, ψ_{qr}	d-q Axes flux Linkages
ψ_m	Mutual Flux Linkage
ψ_r	Rotor Flux Linkage
ψ_s	Stator Flux Linkage
ω_r	Rotor Electrical Speed

ω_s

Synchronous Speed

ω_{sl}

Slip Speed

Appendix C. Listing of Programs

```

C*****
C   THIS PROGRAM SIMULATES THE DYNAMIC CONDITIONS OF AN
C   INDIRECT VECTOR CONTROLLED INDUCTION MOTOR TORQUE DRIVE
C   SYSTEM USING THE SYNCHRONOUSLY ROTATING FRAME
C*****
C   X IS THE STATE VECTOR
C   X(1) = IQS THE QUADRATURE AXIS CURRENT IN THE STATOR
C   X(2) = IQR THE QUADRATURE AXIS CURRENT IN THE ROTOR
C   X(3) = IDS THE DIRECT AXIS CURRENT IN THE STATOR
C   X(4) = IDR THE DIRECT AXIS CURRENT IN THE ROTOR
C   X(5) = M THE SPEED OF THE ROTOR IN ELECTRICAL RAD/SEC
C   X(6) = THETA THE ANGULAR POSITION OF THE ROTOR
C   RS,RR ARE THE STATOR AND ROTOR RESISTANCES
C   LM IS THE MUTUAL INDUCTANCE BETWEEN STATOR AND ROTOR
C   SLL, RLL STATOR AND ROTOR LEAKAGE INDUCTANCES
C   J - MOMENT OF INERTIA , P - NO. OF POLES , MS SYN. FREQ IN RAD/SEC
C   DX - DERIVATIVE OF THE X VECTOR , XEND - VECTOR THAT STORES THE
C   THE LATEST VALUES OF X, XWRK PROVIDES THE WORK AREA FOR RK-METHOD.
C*****
      DIMENSION X(7),DX(7),XEND(7),XWRK(4,7),V(3)
      REAL LM,J,IAS,IBS,ICS,IAC,IBC,ICC
      COMMON RS,RR,LM,SLL,RLL,J,P,MS,V,VQS,VDS,TEMSP,VA
      DO 10 I=1,7
      X(I)=0.0
      DX(I)=0.0
10  CONTINUE
C*****
C   STATE VECTOR IS INITIALISED. FLUX IS 1 PU AND SPEED IS 50R/S
C*****
      X(1) = 16.710
      X(2) = -16.040
      X(3) = 7.6515
      X(4) = -0.024
      X(6) = 85.817
      X(7) = 1.7825
      VQS = 0.0
      VDS = 0.0
      RS=0.277
      RR=0.183
      LM=0.05384
      SLL=0.00145
      RLL=0.00222
      J=0.01667
      X(5) = 50.00
      TEMSP = 50.00
      P=4.0
      TO=0.125
      N=7
      MS=X(5)
      VA=285.0
      VB=0.0
      VC=0.0
      V(1)=95
      V(2)=-190
      V(3)=95.

```

```

MSL=0.0
KOUNT = 0
TP3=2.0*3.1415/3.0
H=5.0E-6
DO 20 I=1,500
CALL RKSYST(TO,H,X,XEND,XWRK,DX,N)
DO 30 JJ=1,N
X(JJ)=XEND(JJ)
30 CONTINUE
TE=0.75*P*(X(1)*X(4)-X(3)*X(2))*LM
PSIRD=LM*X(3)+(LM+RLL)*X(4)
PSIRQ=LM*X(1)+(LM+RLL)*X(2)
PSIR = SQRT (PSIRD**2 + PSIRQ**2)
THETA=X(6)+X(7)
IAS=X(1)*COS(THETA)+X(3)*SIN(THETA)
IBS=X(1)*COS(THETA-TP3)+X(3)*SIN(THETA-TP3)
ICS=X(1)*COS(THETA+TP3)+X(3)*SIN(THETA+TP3)
IF(KOUNT.LE.1) GO TO 101
WRITE(11,14) TO,X(5),PSIR,TE
WRITE(8,14) TO, IAS, IAC
WRITE(9,14) TO,VA
14 FORMAT(1X,4(2X,E15.6))
KOUNT=1
16 FORMAT(1X,5(E10.3,2X))
101 KOUNT=KOUNT+1
CALL INVERH (TO,X,IAS,IBS,ICS,IAC,IBC,ICC)
TO=TO+H
20 CONTINUE
WRITE (10,15) TO,X(1),X(2),X(3),X(4),X(5),X(6),X(7), VQS, VDS,MS
15 FORMAT(3X,4(E16.5,2X),/)
18 FORMAT(3X,3(E16.5,2X))
END
C *****
C THIS SUBROUTINE SOLVES A SYSTEM OF DIFFERENTIAL EQUATIONS USING
C 4TH ORDER RUNGE-KUTTA METHOD
C *****
SUBROUTINE RKSYST(TO,H,XO,XEND,XWRK,F,N)
DIMENSION XO(N),XEND(N),XWRK(4,N),F(N),V(3)
REAL LM,J
COMMON RS,RR,LM,SLL,RLL,J,P,MS,V,VQS,VDS,TEMPSP,VA
CALL DERIVS(XO,TO,F,N)
DO 10 I=1,N
XWRK(1,I)=H*F(I)
XEND(I)=XO(I)+XWRK(1,I)/2.
10 CONTINUE
CALL DERIVS(XEND,TO+H/2.,F,N)
DO 20 JJ=1,N
XWRK(2,JJ)=H*F(JJ)
XEND(JJ)=XO(JJ)+XWRK(2,JJ)/2.
20 CONTINUE
CALL DERIVS(XEND,TO+H/2.,F,N)
DO 30 K=1,N
XWRK(3,K)=H*F(K)
XEND(K)=XO(K)+XWRK(3,K)
30 CONTINUE

```

*TO = 1.125
H = 5e-6*

```

CALL DERIVS(XEND,TO+H,F,N)
DO 40 L=1,N
  XHRK(4,L)=H*F(L)
40 CONTINUE
DO 50 I=1,N
  XEND(I)=XO(I)+(XHRK(1,I)+2.*XHRK(2,I)+2.*XHRK(3,I)+XHRK(4,I))/6
50 CONTINUE
RETURN
END

C
C *****
C THIS SUBROUTINE EVALUATES THE DERIVATIVE VECTOR
C *****
SUBROUTINE DERIVS(Y,T,F,N)
DIMENSION Y(N),F(N),V(3)
REAL LM,J
COMMON RS,RR,LM,SLL,RLL,J,P,MS,V,VQS,VDS,TEMSP,VA
TE=0.75*P*(Y(1)*Y(4)-Y(3)*Y(2))*LM
Y(5) = TEMSP
WSL=MS-Y(5)
PHI1=Y(6)+Y(7)
SSL=SLL+LM
RSL=RLL+LM
TP=2.*3.1415/3.
PHI2=PHI1-TP
PHI3=PHI1+TP
VQS=(2./3.)*(COS(PHI1)*V(1)+COS(PHI2)*V(2)+COS(PHI3)*V(3))
VDS=(2./3.)*(SIN(PHI1)*V(1)+SIN(PHI2)*V(2)+SIN(PHI3)*V(3))
B1=1/(RSL*SSL-LM**2)
X1=VQS-RS*Y(1)-MS*SSL*Y(3)-MS*LM*Y(4)
X2=-RR*Y(2)-MS*LM*Y(3)-MS*RSL*Y(4)
X3=-RS*Y(3)+VDS+MS*SSL*Y(1)+MS*LM*Y(2)
X4=MS*LM*Y(1)+MS*RSL*Y(2)-RR*Y(4)
F(1)=(RSL*X1-LM*X2)*B1
F(2)=(-LM*X1+SSL*X2)*B1
F(3)=(RSL*X3-LM*X4)*B1
F(4)=(-LM*X3+X4*RSL)*B1
F(5)=TE/(2.0*J)
F(6)=Y(5)
F(7)=WSL
RETURN
END

C
C *****
C THIS SUBROUTINE SIMULATES THE INVERTER WITH HYSTERESIS CURRENT
C CONTROLLER
C *****
SUBROUTINE INVERH ( T,X,IA,IB,IC,IAC,IBC,ICC )
COMMON RS,RR,LM,SLL,RLL,J,P,MS,V,VQS,VDS,TEMSP,VA
DIMENSION X(7), V(3)
REAL ITC,IFC,KT,IAC,IBC,ICC,IA,IB,IC,IAE,IBE,ICE,IDEL,MIDEL
REAL LR,LM
PSIRC = 0.412
TEC = 22.0
IDEL = 0.01

```

Y=X?
T=125 *F=125*

WSL=MS-Y(5)
constant

125
125
125
125

B=0.00202

```

TEC = 22.0
IDEL = 0.01
VLK = 285.0
LR = LM + RLL
TR = LR/RR
KT = 0.75 * P * (LM/LR)
ITC = TEC / (KT * PSIRC)
IFC = PSIRC/LM
MSLC = (LM * TEC) / (KT * TR * (PSIRC**2))
THETA = (2. * 3.1415927)/3.
MS = MSLC + X(5)
PHI = X6 + X7
IAC = ITC*COS(PHI) + IFC*SIN(PHI)
IBC = ITC*COS(PHI-THETA) + IFC*SIN(PHI-THETA)
ICC = ITC*COS(PHI+THETA) + IFC*SIN(PHI+THETA)
IAE = IA - IAC
IBE = IB - IBC
ICE = IC - ICC
MIDEL = -(IDEL)
IF (IAE .GT. IDEL) THEN
  VA = -VLK/2.0
ELSEIF (IAE .LT. MIDEL) THEN
  VA = VLK/2.0
ENDIF
IF (IBE .GT. IDEL) THEN
  VB = -VLK/2.0
ELSEIF (IBE .LT. MIDEL) THEN
  VB = VLK/2.0
ENDIF
IF (ICE .GT. IDEL) THEN
  VC = -VLK/2.0
ELSEIF (ICE .LT. MIDEL) THEN
  VC = VLK/2.0
ENDIF
C VAB = VA - VB
C VBC = VB - VC
C VCA = VC - VA
VN = (VA + VB + VC) / 3.
V(1) = VA - VN
V(2) = VB - VN
V(3) = VC - VN
RETURN
END

C
C
C *****
C THIS SUBROUTINE SIMULATES AN INVERTER WITH PWM CURRENT CO
C *****
C SUBROUTINE INVERP ( T,X,IA,IB,IC,IAC,IBC,ICC)
C COMMON RS,RR,LM,SLL,RLL,J,P,WS,V,TEMSP,X6,X7
C DOUBLE PRECISION X(7), V(3)
C DOUBLE PRECISION ITC,IFC,KT,IAC,IBC,ICC,IA,IB,IC, T, H
C DOUBLE PRECISION LM, SLL, RLL, WS, RS, RR, IAE, IBE, ICE
C DOUBLE PRECISION VQS,VDS, VA, VB, VC, RAMCUR
C REAL J, LR

```

```

TEC = 20.0
PSIRC = 0.412
LR = LM + RLL
TR = LR/RR
KT = 0.75 * P * (LM/LR)
ITC = TEC / (KT * PSIRC)
IFC = PSIRC/LM
MSLC = (LM * TEC) / (KT * TR * (PSIRC**2))
THETA = (2. * 3.1415927)/3.
WS = TEMSP + MSLC
PHI = X6 + X7
IAC = ITC*COS(PHI) + IFC*SIN(PHI)
IBC = ITC*COS(PHI-THETA) + IFC*SIN(PHI-THETA)
ICC = ITC*COS(PHI+THETA) + IFC*SIN(PHI+THETA)
25  FORMAT(4(2X,E15.6))
GAIN = 1000.0
IAE = (IAC-IA)*GAIN
IBE = (IBC-IB)*GAIN
ICE = (ICC-IC)*GAIN
PEAK = 24.00
IF (ABS(IAE) .LT. PEAK) GO TO 51
IF (IAE .GE. PEAK) THEN
  IAE = PEAK
ELSE
  IAE = -PEAK
ENDIF
51  IF(ABS(IBE) .LT. PEAK) GO TO 52
IF(IBE .GE. PEAK) THEN
  IBE = PEAK
ELSE
  IBE = -PEAK
ENDIF
52  IF(ABS(ICE) .LT. PEAK) GO TO 53
IF(ICE .GE. PEAK) THEN
  ICE = PEAK
ELSE
  ICE = -PEAK
ENDIF
53  CALL RAMP (T, RAMCUR, SLOPE)
IF (IAE .GT. RAMCUR) THEN
  CST1 = 1.0
ELSE
  CST1 = -1.0
ENDIF
IF (CST1 .EQ. PCST1) GO TO 100
IF (SLOPE .EQ. S1) GO TO 100
S1 = SLOPE
IF (IAE .GT. RAMCUR) THEN
  VA = 142.5
ELSE
  VA = -142.5
ENDIF
100 IF (IBE .GT. RAMCUR) THEN
  CST2 = 1.0
ELSE

```

III

```

      CST2 = -1.0
ENDIF
      IF (CST2 .EQ. PCST2) GO TO 200
      IF (SLOPE .EQ. S2) GO TO 200
      S2 = SLOPE
      IF (IBE .GT. RAMCUR) THEN
      VB = 142.5
      ELSE
      VB = -142.5
      ENDIF
200 IF (ICE .GT. RAMCUR) THEN
      CST3 = 1.
      ELSE
      CST3 = -1.
      ENDIF
      IF (CST3 .EQ. PCST3) GO TO 300
      IF (SLOPE .EQ. S3) GO TO 300
      S3 = SLOPE
      IF (ICE .GT. RAMCUR) THEN
      VC = 142.5
      ELSE
      VC = -142.5
      ENDIF
300 VN = (VA + VB + VC)/ 3.0
      V(1) = VA - VN
      V(2) = VB - VN
      V(3) = VC - VN
      PCST1 = CST1
      PCST2 = CST2
      PCST3 = CST3
C      WRITE(9,41) (V(L), L =1,3), VA,VB,VC
41  FORMAT(1X, 'INVERT', 2X, 3F10.3,/, 'VA', 3F12.3)
C      WRITE(11, 25) T, IC, ICC, VA
C      WRITE(8,25) T, IC
C      WRITE(9,25) T,ICC
      RETURN
      END
*****
*****SUBROUTINE TO GENERATE A RAMP FUNCTION *****
      SUBROUTINE RAMP(T, RAMCUR, SLOPE)
      DOUBLE PRECISION T, A, RAMCUR
      A = DMOD(T,2.50D-4)
      P = 25.00
      IF(A .LE. 1.25E-4) GO TO 20
      RAMCUR =-P + 2*P * (A -1.25E-4)/1.25E-4
      SLOPE = 1
      GO TO 11
20  RAMCUR = P - 2*P* A / 1.25E-4
      SLOPE = -1
11  RETURN
      END

```



```

C*****
C   THIS PROGRAM SIMULATES THE DYNAMIC CONDITIONS OF AN
C   INDIRECT VECTOR CONTROLLED INDUCTION MOTOR SPEED DRIVE SYSTEM
C*****
C   X IS THE STATE VECTOR
C   X(1) = IQS THE QUADRATURE AXIS CURRENT IN THE STATOR
C   X(2) = IQR THE QUADRATURE AXIS CURRENT IN THE ROTOR
C   X(3) = IDS THE DIRECT AXIS CURRENT IN THE STATOR
C   X(4) = IDR THE DIRECT AXIS CURRENT IN THE ROTOR
C   X(5) = W THE ANGULAR ACCELERATION OF THE ROTOR
C   X(6) = THETA THE ANGULAR POSITION OF THE ROTOR
C   RS,RR ARE THE STATOR AND ROTOR RESISTANCES
C   LM IS THE MUTUAL INDUCTANCE BETWEEN STATOR AND ROTOR
C   SLL, RLL STATOR AND ROTOR LEAKAGE INDUCTANCES
C   J - MOMENT OF INERTIA , P - NO. OF POLES , WS SYN. FREQ IN RAD/SEC
C   DX - DERIVATIVE OF THE X VECTOR , XEND - VECTOR THAT STORES THE
C   THE LATEST VALUES OF X, XWRK PROVIDES THE WORK AREA FOR RK-METHOD.
C*****
      DIMENSION X(8),DX(8),XEND(8),XWRK(4,8),V(3)
      REAL LM,J,IAS,IBS,ICS,IAC,IBC,ICC
      COMMON RS,RR,LM,SLL,RLL,J,P,WS,V,VQS,VDS,VA,X8,TEMSP,TEC
      DO 10 I=1,8
      X(I)=0.0
      DX(I)=0.0
10  CONTINUE
C*****
C   INITIALISE THE STATOR VECTOR
C*****
      X(1) = 0.473576
      X(2) = -0.505784E-01
      X(3) = 7.768
      X(4) = -0.12383
      X(5) = 182.0
      X(6) = 31.3493
      X(7) = 2.1955
      X(8) = 0.139044
      VQS = 0.0
      VDS = 0.0
      RS=0.277
      RR=0.183
      LM=0.05384
      SLL=0.00145
      RLL=0.00222
      J=0.01667
      TEMSP = X(5)
      P=4.0
      TO=0.25
      N=8
      WS=X(5)
      VA=285.0
      VB=0.0
      VC=0.0
      V(1)=95
      V(2)=-190
      V(3)=95.

```

```

MSL=0.0
KOUNT = 0
TP3=2.0*3.1415/3.0
H=5.0E-6
DO 20 I=1,25000
CALL RKSYST(TO,H,X,XEND,XWRK,DX,N)
DO 30 JJ=1,N
X(JJ)=XEND(JJ)
30 CONTINUE
TE=0.75*P*(X(1)*X(4)-X(3)*X(2))*LM
PSIRD=LM*X(3)+(LM+RLL)*X(4)
PSIRQ=LM*X(1)+(LM+RLL)*X(2)
PSIR = SQRT (PSIRD**2 + PSIRQ**2)
THETA=X(6)+X(7)
X8 = X(8)
IAS=X(1)*COS(THETA)+X(3)*SIN(THETA)
IBS=X(1)*COS(THETA-TP3)+X(3)*SIN(THETA-TP3)
ICS=X(1)*COS(THETA+TP3)+X(3)*SIN(THETA+TP3)
IF(KOUNT.LE.500) GO TO 101
WRITE(11,14) TO,X(5),PSIR,TE
C WRITE(10,14) TO,IAS, IAC
C WRITE(9,14) TO, TEC
14 FORMAT(1X,4(2X,E15.6))
KOUNT=1
16 FORMAT(1X,5(E10.3,2X))
101 KOUNT=KOUNT+1
CALL INVERH (TO,X,IAS,IBS,ICS,IAC,IBC,ICC)
TO=TO+H
20 CONTINUE
WRITE (14,14) (X(I), I = 1,8),MS
15 FORMAT(3X,4(E16.5,2X),/)
18 FORMAT(3X,3(E16.5,2X))
END

C*****
C THIS SUBROUTINE SOLVES A SYSTEM OF DIFFERENTIAL EQUATIONS USING
C FOURTH ORDER RANGE-KUTTA METHOD.
C*****
SUBROUTINE RKSYST(TO,H,XO,XEND,XWRK,F,N)
DIMENSION XO(N),XEND(N),XWRK(4,N),F(N),V(3)
REAL LM,J
COMMON RS,RR,LM,SLL,RLL,J,P,MS,V,VQS,VDS,VA,X8,TEMSP,TEC
CALL DERIVS(XO,TO,F,N)
DO 10 I=1,N
XWRK(1,I)=H*F(I)
XEND(I)=XO(I)+XWRK(1,I)/2.
10 CONTINUE
CALL DERIVS(XEND,TO+H/2.,F,N)
DO 20 JJ=1,N
XWRK(2,JJ)=H*F(JJ)
XEND(JJ)=XO(JJ)+XWRK(2,JJ)/2.
20 CONTINUE
CALL DERIVS(XEND,TO+H/2.,F,N)
DO 30 K=1,N
XWRK(3,K)=H*F(K)

```

```

        XEND(K)=XO(K)+XWRK(3,K)
30      CONTINUE
        CALL DERIVS(XEND,TO+H,F,N)
        DO 40 L=1,N
            XWRK(4,L)=H*F(L)
40      CONTINUE
        DO 50 I=1,N
            XEND(I)=XO(I)+(XWRK(1,I)+2.*XWRK(2,I)+2.*XWRK(3,I)+XWRK(4,I))/6
50      CONTINUE
        X8 = XEND(8)
        TEMSP = XEND(5)
        RETURN
        END

```

C

C*****

C THIS SUBROUTINE EVALUATES THE DERIVATIVE VECTOR

C*****

```

SUBROUTINE DERIVS(Y,T,F,N)
DIMENSION Y(N),F(N),V(3)
REAL LM,J
COMMON RS,RR,LM,SLL,RLL,J,P,WS,V,VQS,VDS,VA,X8,TEMSP,TEC
TE=0.75*P*(Y(1)*Y(4)-Y(3)*Y(2))*LM
TL = 19.5
WRC =50.00
WSL=WS-TEMSP
PHI1=Y(6)+Y(7)
SSL=SLL+LM
RSL=RLL+LM
TP=2.*3.1415/3.
PHI2=PHI1-TP
PHI3=PHI1+TP
VQS=(2./3.)*(COS(PHI1)*V(1)+COS(PHI2)*V(2)+COS(PHI3)*V(3))
VDS=(2./3.)*(SIN(PHI1)*V(1)+SIN(PHI2)*V(2)+SIN(PHI3)*V(3))
B1=1/(RSL*SSL-LM**2)
X1=VQS-RS*Y(1)-WS*SSL*Y(3)-WS*LM*Y(4)
X2=-RR*Y(2)-WSL*LM*Y(3)-WSL*RSL*Y(4)
X3=-RS*Y(3)+VDS+WS*SSL*Y(1)+WS*LM*Y(2)
X4=WSL*LM*Y(1)+WSL*RSL*Y(2)-RR*Y(4)
F(1)=(RSL*X1-LM*X2)*B1
F(2)=(-LM*X1+SSL*X2)*B1
F(3)=(RSL*X3-LM*X4)*B1
F(4)=(-LM*X3+X4*RSL)*B1
F(5)=(TE-TL)*2.0/J
F(6)=Y(5)
F(7)=WSL
F(8) = 0.01 * (WRC - TEMSP)
RETURN
END

```

C

C*****

C THIS SUBROUTINE SIMULATES THE INVERTVER WITH HYSTERESIS CURRENT
C CURRENT CONTROL.

C*****

```

SUBROUTINE INVERH ( T,X,IA,IB,IC,IAC,IBC,ICC )
COMMON RS,RR,LM,SLL,RLL,J,P,WS,V,VQS,VDS,VA,X8,TEMSP,TEC

```

```

DIMENSION X(8), V(3)
REAL ITC,IFC,KT,IAC,IBC,ICC,IA,IB,IC,IAE,IBE,ICE,IDEL,MIDEL
REAL LR,LM
WRC =50.00
PSIRC = 0.412
TEC = 25.0*(WRC - TEMSP) + X8

C
C TORQUE IS LIMITED TO +2PU AND -2PU
C

IF (TEC .GT. 40.0) THEN
TEC = 40.0
GO TO 31
ELSE
GO TO 31
ENDIF
31 IF (TEC .LT. -40.0) THEN
TEC = -40
GO TO 32
ELSE
GOTO 32
ENDIF
32 IDEL = 0.01
VLK = 285.0
LR = LM + RLL
TR = LR/RR
KT = 0.75 * P * (LM/LR)
ITC = TEC / (KT * PSIRC)
IFC = PSIRC/LM
WSLC = (LM * TEC) / (KT * TR * (PSIRC**2))
THETA = (2. * 3.1415927)/3.
WS = WSLC + X(5)
PHI = X(6) + X(7)
IAC = ITC*COS(PHI) + IFC*SIN(PHI)
IBC = ITC*COS(PHI-THETA) + IFC*SIN(PHI-THETA)
ICC = ITC*COS(PHI+THETA) + IFC*SIN(PHI+THETA)
IAE = IA - IAC
IBE = IB - IBC
ICE = IC - ICC
MIDEL = -(IDEL)
IF (IAE .GT. IDEL) THEN
VA = -VLK/2.0
ELSEIF (IAE .LT. MIDEL) THEN
VA = VLK/2.0
ENDIF
IF (IBE .GT. IDEL) THEN
VB = -VLK/2.0
ELSEIF (IBE .LT. MIDEL) THEN
VB = VLK/2.0
ENDIF
IF (ICE .GT. IDEL) THEN
VC = -VLK/2.0
ELSEIF (ICE .LT. MIDEL) THEN
VC = VLK/2.0
ENDIF
VAB = VA - VB

```

```

VBC = VB - VC
VCA = VC - VA
VN = (VA + VB + VC) / 3.
V(1) = VA - VN
V(2) = VB - VN
V(3) = VC - VN
RETURN
END

```

```

C
C*****
C THIS SUBROUTINE SIMULATES AN INVERTER WITH PWM CURRENT CONTROLLER
C*****
SUBROUTINE INVERP ( T,X,IA,IB,IC,IAC,IBC,ICC,V,TEC )
COMMON RS,RR,LM,SLL,RLL,J,P,WS,TEMP, X6, X7, X8, VA
DOUBLE PRECISION X(8), V(3)
DOUBLE PRECISION ITC,IFC,KT,IAC,IBC,ICC,IA,IB,IC, T, H
DOUBLE PRECISION LM, SLL, RLL, WS, RS, RR, IAE, IBE, ICE
DOUBLE PRECISION VQS,VDS, VA, VB, VC, RAMCUR
REAL J, LR
WRC = 182.00
TEC = 50.*(WRC - TEMP) + X8
IF(TEC .GT. 40.0) THEN
TEC = 40.0
ELSE
GO TO 31
ENDIF
31 IF (TEC .LT. -40.0) THEN
TEC = -40.0
ELSE
GO TO 32
ENDIF
32 PSIRC = 0.412
LR = LM + RLL
TR = LR/RR
KT = 0.75 * P * (LM/LR)
ITC = TEC / (KT * PSIRC)
IFC = PSIRC/LM
WSLC = (LM * TEC) / (KT * TR * (PSIRC**2))
THETA = (2. * 3.1415927)/3.
WS = TEMP + WSLC
PHI = X6 + X7
IAC = ITC*COS(PHI) + IFC*SIN(PHI)
IBC = ITC*COS(PHI-THETA) + IFC*SIN(PHI-THETA)
ICC = ITC*COS(PHI+THETA) + IFC*SIN(PHI+THETA)
25 FORMAT(4(2X,E15.6))
GAIN = 1000.0
IAE = (IAC-IA)*GAIN
IBE = (IBC-IB)*GAIN
ICE = (ICC-IC)*GAIN
PEAK = 24.00
IF (ABS(IAE) .LT. PEAK) GO TO 51
IF (IAE .GE. PEAK) THEN
IAE = PEAK
ELSE
IAE = -PEAK

```

```

        ENDIF
51  IF (ABS(IBE) .LT. PEAK) GO TO 52
    IF (IBE .GE. PEAK) THEN
        IBE = PEAK
    ELSE
        IBE = -PEAK
    ENDIF
52  IF (ABS(ICE) .LT. PEAK) GO TO 53
    IF (ICE .GE. PEAK) THEN
        ICE = PEAK
    ELSE
        ICE = -PEAK
    ENDIF
53  CALL RAMP (T, RAMCUR, SLOPE)
    IF (IAE .GT. RAMCUR) THEN
        CST1 = 1.0
    ELSE
        CST1 = -1.0
    ENDIF
        IF (CST1 .EQ. PCST1) GO TO 100
            IF (SLOPE .EQ. S1) GO TO 100
                S1 = SLOPE
                IF (IAE .GT. RAMCUR) THEN
                    VA = 142.5
                ELSE
                    VA = -142.5
                ENDIF
100  IF (IBE .GT. RAMCUR) THEN
        CST2 = 1.0
    ELSE
        CST2 = -1.0
    ENDIF
        IF (CST2 .EQ. PCST2) GO TO 200
            IF (SLOPE .EQ. S2) GO TO 200
                S2 = SLOPE
                IF (IBE .GT. RAMCUR) THEN
                    VB = 142.5
                ELSE
                    VB = -142.5
                ENDIF
200  IF (ICE .GT. RAMCUR) THEN
        CST3 = 1.
    ELSE
        CST3 = -1.
    ENDIF
        IF (CST3 .EQ. PCST3) GO TO 300
            IF (SLOPE .EQ. S3) GO TO 300
                S3 = SLOPE
                IF (ICE .GT. RAMCUR) THEN
                    VC = 142.5
                ELSE
                    VC = -142.5
                ENDIF
300  VN = (VA + VB + VC) / 3.0
    V(1) = VA - VN

```

```

V(2) = VB - VN
V(3) = VC - VN
PCST1 = CST1
PCST2 = CST2
PCST3 = CST3
C   WRITE(9,41) (V(L), L =1,3), VA,VB,VC
41  FORMAT(1X, 'INVERT', 2X, 3F10.3,/, 'VA', 3F12.3)
C   WRITE(11, 25) T, IC, ICC, VA
C   WRITE(8,25) T, IC
C   WRITE(9,25) T,ICC
    RETURN
    END
*****
*****SUBROUTINE TO GENERATE A RAMP FUNCTION *****
SUBROUTINE RAMP(T, RAMCUR, SLOPE)
DOUBLE PRECISION T, A, RAMCUR
A = DMOD(T,2.50D-4)
P = 25.00
IF(A .LE. 1.25E-4) GO TO 20
RAMCUR = -P + 2*P * (A -1.25E-4)/1.25E-4
SLOPE = 1
GO TO 11
20 RAMCUR = P - 2*P* A / 1.25E-4
SLOPE = -1
11 RETURN
    END

```

**The vita has been removed from
the scanned document**